MINERAL PROVINCES 30

AGSO
AUSTRALIAN GEOLOGICAL SURVEY ORGANISATION

The relationship between gold mineralisation and metamorphic grade in the Menzies-Kambalda area, Eastern Goldfields, W.A.: Evidence from fluid inclusions

by T Mernagh and W Witt

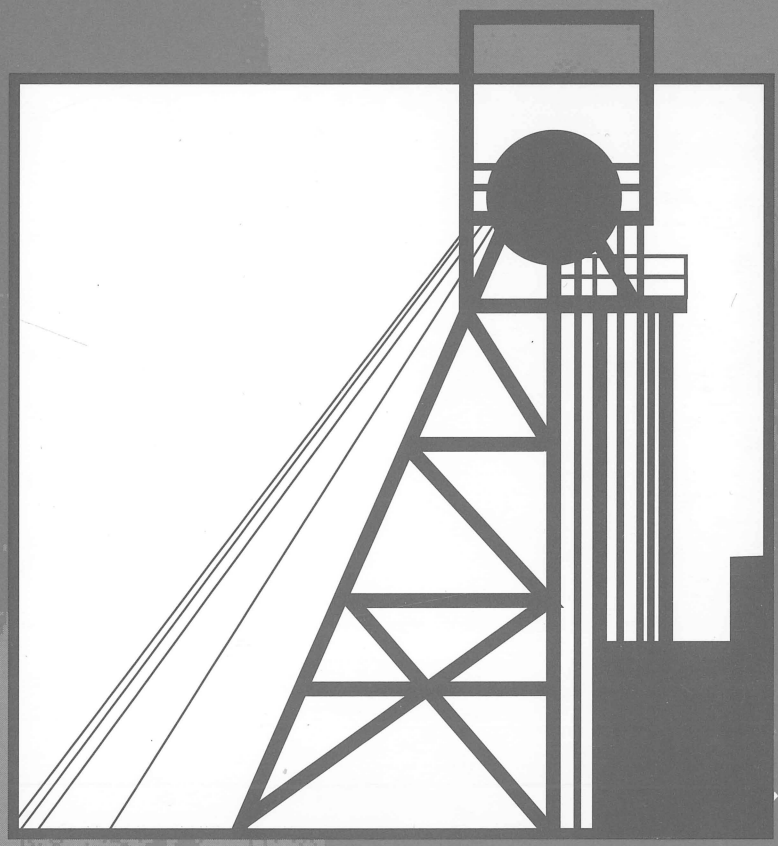

Record 1993/27

MINERALS AND LAND USE PROGRAM

AUSTRALIAN GEOLOGICAL SURVEY ORGANISATION

AGSO

AUSTRALIAN GEOLOGICAL SURVEY ORGANISATION

The Relationship Between Gold Mineralization and Metamorphic Grade in the Menzies—Kambalda Area, Eastern Goldfields, WA: Evidence From Fluid Inclusions

Record 1993/27

T.P. Mernagh[1] and W.K. Witt[2]

1. Australian Geological Survey Organisation
2. Geological Survey of Western Australia

DEPARTMENT OF PRIMARY INDUSTRIES AND ENERGY

Minister for Resources: The Hon. Michael Lee

Secretary: Greg Taylor

AUSTRALIAN GEOLOGICAL SURVEY ORGANISATION
(formerly BUREAU OF MINERAL RESOURCES, GEOLOGY AND GEOPHYSICS)

Executive Director: Roye Rutland

ISSN 1039–0073

ISBN 0 642 19274 X

Contents

SUMMARY

This research forms part of the Eastern Goldfields NGMA project undertaken jointly by the Australian Geological Survey Organisation and the Geological Survey of WA. The National Geoscience Mapping Accord, endorsed by the Australian (now Australian and New Zealand) Minerals and Energy Council in August 1990, is a joint Commonwealth/State/Territory initiative to produce, using modern technology, a new generation of geoscientific maps, data sets, and other information on strategically important regions of Australia over the next 20 years.

This study focuses on Australia's premier gold producing district, the Menzies—Kalgoorlie —Kambalda area, and was aimed at investigating variations in the composition of the ore-forming fluids with changing temperature/metamorphic grade of the gold deposits.

Gold is precipitated from hydrothermal fluids by changes in the ore fluid chemistry, pressure or temperature. These changes can result from a number of physical processes, including:

- interaction between ore fluids and their surrounding host rocks,
- phase separation in response to a pressure decrease during the ascent of the fluid,
- the mixing of two or more different fluids.

Evidence of the above processes can be obtained from the study of fluid inclusions, and hence, fluid inclusions in vein quartz and gangue minerals were selected for study from a reconnaissance of 13 gold deposits in this area. The selected deposits contain alteration assemblages which formed at temperatures ranging from 300 to 600°C. The fluid inclusions are typically less than 15 μm in diameter but range up to 50 μm diameter and eight different types of inclusions have been recognised. The composition and densities of the trapped fluids were determined by microthermometry and analysis with the laser Raman microprobe.

Although fluid compositions varied markedly within and between deposits, CO_2 was present in all assemblages forming at temperatures up to 500°C. N_2 and CH_4 were also abundant in the vapour phase of aqueous inclusions formed at low temperatures while some inclusions forming at temperatures from 500 to 600°C contained only CH_4 in the vapour phase. Similar trends in fluid composition are observed for assemblages forming at temperatures up to 500°C but the assemblage formed at around 600°C is characterised by its lack of CO_2.

Most of the fluid inclusions from the assemblages formed between 300 and 500°C contain relatively high concentrations of CO_2 (up to 60 wt %) which indicates that phase separation may have occurred with the subsequent loss of the aqueous phase. The varying CH_4 content of the fluids suggests that there has been mixing between a CO_2-rich fluid and a CH_4-rich fluid. The CH_4-rich fluid may have been generated by metamorphic devolatilisation reactions in the carbonaceous black shales which are common as interflow sedimentary units in the greenstones of the Menzies—Kambalda area. The low CO_2 content of the fluids for the assemblage formed at 600°C suggest either a change in the style of mineralisation or quite different redox conditions at this temperature.

This was a reconnaissance study based on a limited number of samples but the above observations suggest a model involving deep-seated, CO_2-rich (ore-bearing?) fluids. As these fluids ascend to the surface they undergo phase separation and mix with a reduced wallrock/metamorphic fluid to generate a CO_2/CH_4-rich fluid. Both the possibility of fluid mixing and increasing fluid immiscibility with increasing methane content have important implications for the mechanisms of gold deposition in this region.

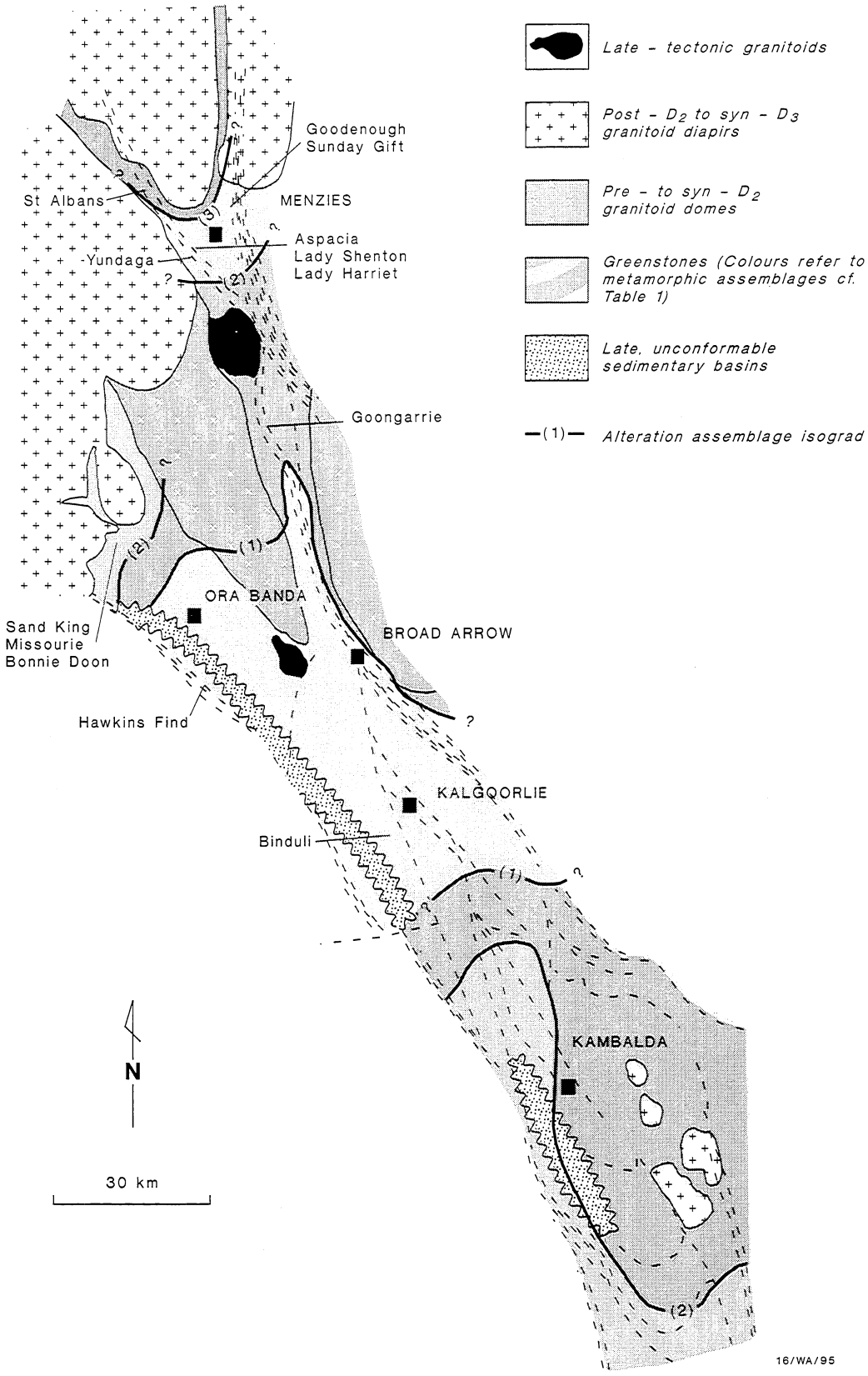

Figure 1. Distribution of alteration assemblages in mineralised mafic rocks in the Menzies—Kambalda area (c.f. Table 1). The heavy lines represent the approximate location of the equilibrium alteration isograds for reactions 1,2, and 3 (see text). The location of deposits examined in this study are also shown on this figure.

INTRODUCTION

The Menzies—Kalgoorlie—Kambalda area (Figure 1) in the Eastern Goldfields has yielded 1700 t of gold, almost one quarter of Australia's total production. Clarke *et al.* (1986, 1988) showed that zoned alteration assemblages at the Victory—Defiance mine, Kambalda, were controlled by increasing X_{CO_2} of the hydrothermal fluid towards centres of the mineralized structures. Zoned alteration assemblages which reflect increasing X_{CO_2} and addition of potassium towards the centres of mineralized structures occur at most deposits in the Menzies—Kambalda area, but the mineralogy of these assemblages also varies on a regional scale, with host rock lithology and metamorphic grade. Regional variation of alteration assemblages with increasing metamorphic grade is best displayed by the metamorphic and metasomatic assemblages associated with mineralization in the mafic rocks (see Table 1).

Phillips (1986) documented alteration patterns associated with the Golden Mile deposits in greenschist facies doleritic rocks at Kalgoorlie. The metamorphic assemblage passes through a chlorite-carbonate-albite assemblage into an inner assemblage consisting of sericite-ankerite-pyrite. These patterns are repeated with minor variations in other Fe-rich mafic-hosted deposits in low to mid greenschist facies metamorphic domains (e.g. Mt Pleasant, Ora Banda, Grants Patch). Zoned alteration assemblages about individual mineralized structures in lower amphibolite grade mafic rocks at the Victory—Defiance mine, Kambalda, consist of an outer zone containing biotite-chlorite-calcite-sphene and an inner zone characterized by a quartz-albite-ankerite-muscovite-pyrite-rutile assemblage (Clark *et al.*, 1986, 1988). Similar alteration assemblages have been documented at the Hunt mine (Phillips and Groves, 1984) and other deposits in the Kambalda area (Cowden and Roberts, 1990) as well as at New Mexico, Wycheproof and Goongarrie.

Chlorite, muscovite and ankerite are absent from metasomatic assemblages in slightly higher metamorphic grade domains such as Siberia and Menzies. In these areas, foliation-controlled biotitisation of amphibolite increases in intensity towards the centre of the mineralized structure where biotite-calcic plagioclase (± quartz, carbonate, sulphides) assemblages are typical. Calcite, which is commonly present as a minor component, is the characteristic carbonate in these deposits. At the highest metamorphic grade (e.g. St. Albans), the inner most alteration zones are characterized by diopside, garnet and microcline. Minimum temperatures of approximately 560°C for the formation of this assemblage are suggested by experimental constraints on the breakdown of biotite-calcite-quartz to give K-feldspar + tremolite (Hoschek, 1973).

The distribution of the four parageneses identified in Table 1 is shown in Figure 1 and supports a relationship between alteration assemblages and regional metamorphic grade. Potassium metasomatism is manifest as muscovite, biotite, and microcline in progressively higher metamorphic grade domains. The boundaries between domains characterized by the four alteration parageneses can be represented by the following isograds:

$$\underset{\text{muscovite}}{KAl_3Si_3O_{10}OH_2} + \underset{\text{ankerite}}{9CaFe(CO_3)_2} + \underset{\text{quartz}}{6SiO_2} + 2K^+ + 3H_2O = \underset{\text{biotite}}{3KFe_3AlSi_3O_{10}(OH)_2} + \underset{\text{calcite}}{9CaCO_3} + 9CO_2 + 2H^+ \quad (1)$$

$$\underset{\text{ankerite}}{CaFe(CO_3)_2} + \underset{\text{chlorite}}{Fe_5Al_2Si_3O_{10}(OH)_8} + 2H^+ = \underset{\text{anorthite}}{CaAl_2Si_2O_8} + \underset{\text{quartz}}{SiO_2} + 6Fe^{2+} + 2CO_2 + 10OH^- \quad (2)$$

$$\underset{\text{biotite}}{KMg_3AlSi_3O_{10}(OH)_2} + \underset{\text{calcite}}{3CaCO_3} + 6SiO_2 = \underset{\text{microcline}}{KAlSi_3O_8} + \underset{\text{diopside}}{3CaMgSi_2O_6} + 3CO_2 + H_2O \quad (3)$$

TABLE 1. METAMORPHIC AND METASOMATIC ASSEMBLAGES ASSOCIATED WITH MINERALISATION IN MAFIC ROCKS IN THE MENZIES— KAMBALDA AREA

	Inner alteration zone	Outer alteration zone	Metamorphic assemblage	Examples
600°C (4)	Microcline Diopside Garnet Calcic Plagioclase Calcite Pyrrhotite Pyrite Arsenopyrite	Hornblende Calcic Plagioclase Biotite Calcite Sphene Pyrrhotite	Hornblende Calcic Plagioclase Ilmenite	St Albans
500°C (3)	Quartz Biotite Calcic Plagioclase Sphene Pyrrhotite Pyrite Arsenopyrite	Biotite Hornblende Calcic Plagioclase Calcite Garnet Ilmenite Pyrrhotite Pyrite	Hornblende Calcic Plagioclase Ilmenite	Aspacia Lady Shenton Lady Harriet Yundaga Goodenough Sunday Gift Bonnie Doon Missouri Sand King
400°C (2)	Quartz Ankerite Albite Muscovite Rutile Pyrite	Biotite/Chlorite Calcite Sphene Epidote Pyrrhotite Pyrite	Actinolite or Hornblende Albite or Calcic Plagioclase Ilmenite ± Epidote	Goongarrie
300°C (1)	Muscovite Ankerite Siderite Pyrite Pyrrhotite Arsenopyrite	Chlorite Calcite or Ankerite Albite Epidote Ilmenite Pyrrhotite	Actinolite Albite Ilmenite ± Epidote	Hawkins Find Binduli

Modified from Witt (1991)

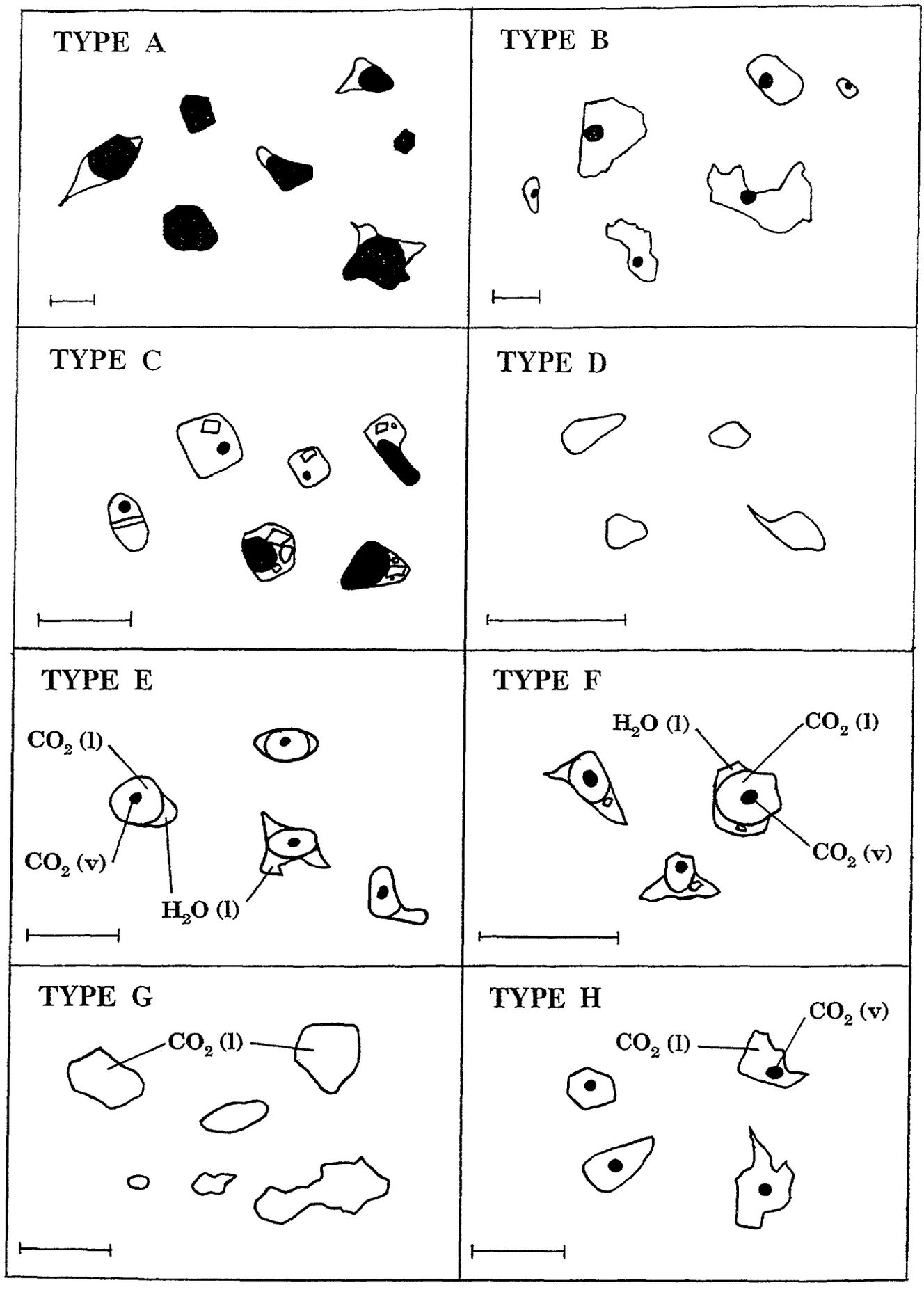

Figure 2. Schematic representation of fluid inclusions types observed in the Menzies—Kambalda area. Vapour phases are shown in black. Scale bars represent 10 μm.

Alteration assemblages associated with gold deposits in the Menzies—Kambalda area suggest the involvement of hydrothermal fluids containing significant amounts of CO_2 and potassium. The relations among mineralisation, alteration assemblages, and metamorphic grade, and the synmetamorphic granitoids suggest that the mineralising event was related to a large, greenstone belt-scale, hydrothermal system centered on the cooling plutons (Witt, 1991). A study of fluid inclusions from selected deposits of varying metamorphic grade in the Menzies—Kambalda area has been carried out to further investigate the nature of the hydrothermal system. The samples also included strongly albitized porphyry which hosts gold mineralisation at Binduli and Hawkins Find which were investigated in order to document the nature of the albitising fluids.

ANALYTICAL PROCEDURES

Doubly polished sections were prepared from quartz ± carbonate ± albite veins in mineralised zones from each of the selected deposits. Suitable sections were then studied by microthermometry. The observation of depressed CO_2 melting temperatures indicated that methane or other gases were present in most inclusions. Many inclusions contained only CO_2 ± CH_4 with no observable aqueous phase (although 10-15 vol.% H_2O may be present as a thin film on the walls of the inclusions). Some of these inclusions contained a liquid and vapour phase at room temperature while others only formed a vapour phase on cooling. Due to the low melting point of methane (-182.5°C) the inclusions could not be completely frozen and solid CO_2 was not observed in the CH_4-rich inclusions. Homogenisation of the liquid and vapour phases occurs before the critical point which is at -82.6°C for pure CH_4 and 31.1°C for pure CO_2. Hence, CO_2 - CH_4 mixtures may homogenise at any temperature up to 31°C but CO_2 or CH_4 dominant fluids tend to homogenise close to their respective critical points.

The presence of methane also prevents the estimation of salinity from the clathrate melting temperatures and the densities given for CO_2-rich inclusions in the following tables are calculated from the homogenisation temperatures for CO_2 but neglect the effect of any methane in the inclusion. Raman spectroscopy was also carried out on selected, individual inclusions to quantify the relative amounts of each species in the carbonic phase and to identify some of the daughter solids in some inclusions.

Abundant fluid inclusions were observed in most of the veins that were sampled and they ranged in size from less than 1 μm to 50 μm but were typically less than 10 μm. It should be noted that the maximum size of inclusions varies between deposits and is strongly dependent upon the nature and severity of post-trapping deformation. Eight different types of fluid inclusions are defined on the basis of appearance at room temperature and the fluid composition. They are shown diagramatically in Figure 2 and are tabulated below:

Key to Fluid Inclusion Types

Type A = Vapour rich (commonly with >25 vol.% vapour) aqueous inclusions

Type B = Undersaturated (L + V) aqueous inclusions

Type C = Saturated inclusions (contains one or more solids)

Type D = Monophase aqueous inclusions

Type E = 3 phase H_2O - CO_2 inclusions containing (L + V) CO_2

Type F = Multiphase H_2O - CO_2 inclusions containing (L + V) CO_2 + solids

Type G = Monophase carbonic (generally CO_2-rich) inclusions with no observable aqueous phase

Type H = Two phase (L + V) carbonic inclusions with no observable aqueous phase

RESULTS

The results will be presented in order of increasing metamorphic grade and in relation to the alteration assemblages outlined in Table 1 and Figure 1. The complete set of microthermometric data for each deposit is presented in Appendix A and the Raman spectroscopic data for selected deposits is presented in Appendix B.

Gold Deposits Associated with Alteration Assemblage 1

BINDULI

Production: Binduli is a small mining centre with a total production of 359.8 t ore for 7.17 kg gold at 19.9 g/t (1897 - 1942). Open pit resources are 716,000 t at 1.89 g/t (1,356 kg gold) from four deposits.

Host Rocks: Albite-rich feldspar porphyry. Dacitic to rhyolitic volcaniclastic metasediments of the Black Flag Group are a minor host rock.

Mineralised Structures: (1) A stockwork of quartz veining dominated by flat-lying vein sets in porphyry. Similar flat-lying quartz veins dip south in adjacent volcaniclastic sediments.

(2) Steep 150-160° trending shear zones with some quartz veining, particularly along porphyry/volcaniclastic rock contacts. These shears dip 70°W to 80°E.

(3) Subvertical E-W faults with small dextral (<50 m) offsets.

Flat quartz ± sulfide veins are terminated but not offset by steep, strike-parallel shears.

Alteration: Well foliated volcaniclastic rocks are pervasively sericitised, carbonated and pyritised over a broad interval (tens of metres?) either side of the porphyry. Minor amounts of secondary tourmaline and chlorite are also present. Hematite also occurs as fine, discontinuous trails in the plane of foliation. Irregular, and locally abundant, disseminated secondary magnetite grows over the sericitic fabric and associated hematite. The mineralised porphyry is pervasively albitised and cut by albite-ankerite veinlets. Disseminated ankerite and pyrite with minor but significant galena and chalcopyrite overprint albitisation. There is no distinct alteration halo adjacent to the flat to shallow-dipping mineralised quartz veins.

Inclusion Petrography: The polished sections contained quartz-albite-carbonate veins cutting porphyry with feldspar phenocrysts up to 5mm in diameter. Abundant small inclusions were observed in the vein quartz (<1-30 μm) and calcite (<1-10 μm). The inclusions have irregular to negative crystal shapes and most appear to be pseudosecondary or secondary. Most inclusions contained only CO_2 either as a single phase (Type G) or as liquid and vapour (Type H). Three phase (Type E) inclusions were less abundant and showed variable CO_2 to water ratios.

Microthermometry: Microthermometric data indicate that the inclusions contain only CO_2 and water. Clathrate melting temperatures indicate a salinity of 4-5 eq. Wt% NaCl for Type E inclusions. Mostly the CO_2 phases homogenised at temperatures ranging from 12 to 30°C giving corresponding CO_2 densities of 0.84 to 0.58 g/cm^3 but a few denser fluid inclusions homogenised between 2 and 8°C with corresponding densities of 0.88 to 0.91 g/cm^3.

HAWKINS FIND

Production: Negligible historic production, but open pit mining of 300,000 t of ore at 1.6 g/t produced 480 kg of gold in the period 1985-1987 (unpublished Mines Department figures).

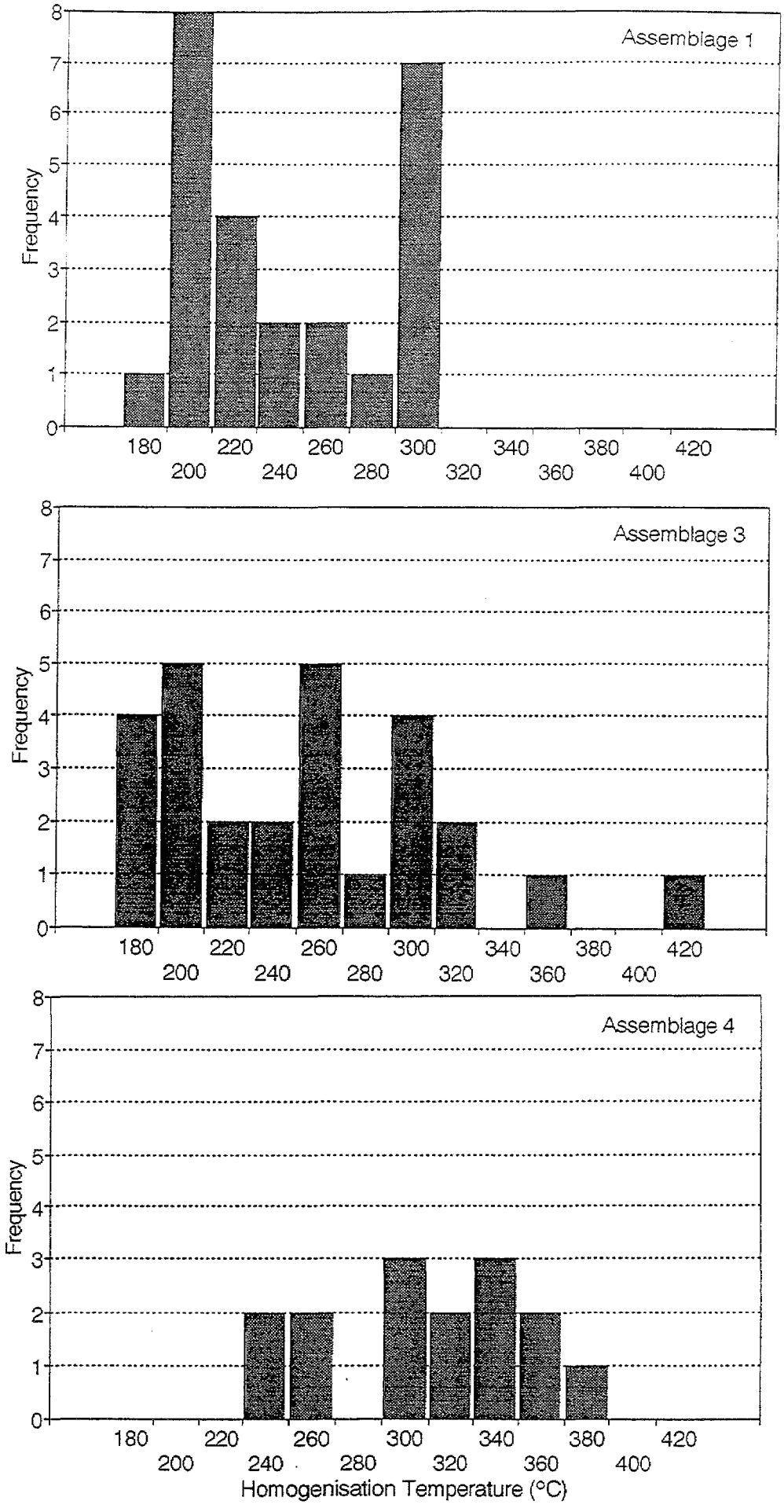

Figure 3. Homogenisation temperatures *l+v(l)* for various assemblages as described in Table 1. Note that solid crystals in Type C inclusions did not dissolve over the temperature range shown in this figure (see text for details).

Host Rocks: Mainly albite-rich porphyry within komatiitic volcanics, and to a lesser extent, komatiitic rocks.

Mineralised Structure: Mineralised zones are associated with shearing at or near NW to NNW-trending contacts between porphyry and ultramafic rocks. Porphyry and shear zones dip about 60°W to subvertical. The porphyry is only weakly foliated but is cut by many irregular to sheeted quartz-ankerite (± biotite ± sulfide) veins which are dominantly east-west and subvertical. Intense veining has caused some local brecciation of the porphyry.

Alteration: Deformed ultramafic rocks in the Zuleika Shear Zone are altered to talc-chlorite-carbonate schist which is overprinted by coarse talc-carbonate ± sulfides (trace to 2% pyrite) in mineralised shears associated with prophyry contacts. Albite in the porphyry is variably recrystallised but albite also occurs in late quartz veins and vughs, indicating that at least some albitic fluids were present during late stages of deformation. Potassic alteration overprints albitisation but the two alteration types also occur independently of each other. Potassic alteration formed irregular veinlets and disseminations of biotite, carbonate (ankerite) and sulfides. The sulfides are dominantly pyrite (variably altered to marcasite) and arsenopyrite, with minor pyrrhotite, sphalerite, chalcopyrite and galena. Minor ilmenite, sphene and scheelite are also associated with mineralised assemblages and were probably introduced during potassic alteration.

Inclusion Petrography: Polished sections contained quartz and calcite crystals in a vugh with albite around the margin of the vugh. This sample has abundant large and possibly primary inclusions (<1-50 μm) in the quartz and trails of smaller inclusions (<1-10 μm) in the albite. The inclusions have irregular to negative crystal shapes and most appear to be pseudosecondary or secondary. Types B, C and D inclusions were observed in quartz but only Type B were observed in albite. Type B inclusions in quartz contained 5-10 vol.% vapour while Type B inclusions in albite contained 20-25 vol.% vapour.

Microthermometry: The microthermometric data is tabulated in Appendix A and is also shown in Figure 3. The type B and C inclusions in quartz contain 5-7 eq. Wt% NaCl and homogenise at temperatures between 180 and 241°C and are thought to be later than the inclusions in albite which homogenised between 278 and 297°C. The secondary inclusions have similar homogenisation temperatures to the primaries in the quartz crystals.

Raman Spectrometry: Only CO_2 could be detected in the Raman spectra recorded from the inclusions in albite. Raman spectra recorded from the inclusions in quartz showed the presence of CO_2, N_2 and CH_4 in the gas phase in varying proportions. Some inclusions contained almost equal amounts of CO_2 and CH_4 with minor N_2 while others contained mostly CH_4 or $CH_4 + N_2$. Raman spectra were also recorded from some of the solids in the Type C inclusions and $BaCO_3$ and some unknown silicate phases were detected.

Gold Deposits Associated with Alteration Assemblage 2

GOONGARRIE

Production: Past production was more than 800 kg of gold, extracted predominantly from the New Boddington mine from 1893 to 1942. New Boddington also contained an open pit resource of 1,526.68 kg of gold from 368,240 t of ore at 4.14 g/t and total production from the Goongarrie mines is estimated to be 4.2 t of gold.

Host Rocks: Basalt, dolerite and quartz-dolerite of the low-Mg series (Bent Tree Basalt).

Mineralised Structures: Gold mineralisation is associated with zones of intense quartz veining and quartz-carbonate-biotite alteration, and particularly with arsenopyrite-rich assemblages. Historic

production was derived from WNW-trending Boddington and Kerman's quartz-sulfide vein systems which are several metres thick and dip 70-75°SW. Open pit production at New Boddington was based on mineralisation in a strike-parallel shear zone which trends 345° and dips 70-80°, and more importantly, on a sheeted and stockwork quartz vein system in the area of intersection between this shear zone and the Boddington-Kerman's vein system. Highest ore grades are commonly located in the acute angle between the quartz-sulfide lodes and the strike-parallel shear zone. Orientations of quartz veins within the stockwork mirror larger-scale structures in the Goongarrie area although they tend to be more flat lying at New Boddington.

Alteration: Strike-parallel shear zones and pervasively foliated mafic rocks are characterised by schistosity-controlled alteration. Anastomosing zones and lenses of plagioclase-carbonate(calcite)-biotite alteration occur within broader zones of carbonate-chlorite alteration. Chlorite rich assemblages generally contain minor disseminated pyrrhotite while biotite-rich assemblages commonly contain larger amounts of pyrite. Both sulfides occur as irregular, elongate, schistosity-controlled disseminations but may also occur in small (≤0.3 mm) "clots" of unoriented pyrite, pyrrhotite, biotite, chlorite and carbonate(calcite). The "clots" are most common towards the inner margin of the carbonate-chlorite alteration zones indicating that potassic alteration locally outlasted ductile deformation.

Rocks characterised by the biotite-rich assemblage are locally brecciated and the interclast spaces are filled with coarse, unoriented chlorite, biotite, sericite, carbonate and sulfides (pyrrhotite and pyrite). Sheeted and stockwork quartz (± minor calcite, biotite, chlorite and sulfides) veins are particularly common in biotite-rich assemblages. Coarse, idioblastic arsenopyrite occurs adjacent to many of these veins. Narrow selvages of albitisation and sericitisation occur adjacent to some quartz veins and are superimposed on the dominant schistosity-controlled alteration. Sericite-albite (± chlorite) assemblages also occur in rare, late, retrograde shear zones, generally subparallel to the dominant shear fabric.

Inclusion Petrography: The polished section contained a 2-3 mm quartz-calcite tension gash in biotite-sulfide rich host rock. Abundant small (<1-20 μm) inclusions were observed in the quartz but none were observed in the calcite. The inclusions are irregular to rounded and appear pseudosecondary or secondary. Only Types G and H were observed and thus no aqueous phases were apparent at room temperature.

Microthermometry: Microthermometric analyses showed slightly depressed T_mCO_2 values but no other gases (apart from CO_2) could be detected by Raman microprobe analysis (see below). The 2 phase inclusions homogenised at temperatures between 16 and 23°C giving corresponding densities of 0.81 to 0.73 g/cm^3.

Raman Spectrometry: As mentioned above, only CO_2 could be detected in the one phase and two phase inclusions. The microthermometric results indicate that other gases are present but their concentrations must be less than a few mole percent.

Gold Deposits Associated with Alteration Assemblage 3

SAND KING

Production: No significant production has been recorded prior to 1980. Modern open pit resources (mined production plus remaining reserves) are approximately 4,157 kg of gold from 1,120,000 t at 4 g/t. Furthermore, there is an underground resource of 4,500 kg of gold from 1,500,000 t of ore at 3 g/t.

Host Rocks: Weakly plagioclase-phyric, low-Mg series (Missouri) basalt.

Mineralised Structure: Mineralisation is hosted by zones of quartz ± biotite ± pyrite veining and brecciation which trend 090-060° and dip 70-80°N. Individual quartz veins vary from 1 mm to <5 m and the *en echelon* arrangement of the quartz veining define a broad 050° trend. Best grades occur in the basaltic rocks adjacent to the porphyry intrusions and at the intersections of the mineralised zone with 010-345° trending faults.

Alteration: Gold occurs in the margins of the quartz ± biotite ± pyrite veins and in the 0.5 - 2 m wide biotite-plagioclase-pyrite (± pyrrhotite) alteration assemblage adjacent to the vein systems. Gold occurs mainly as inclusions and in fractures within pyrite. Other sulfides (galena, chalcopyrite, sphalerite) and tellurides (hessite, petzite, altaite, tellurobismutherite, melonite, freibergite), and scheelite occur in minor quantities. Quartz-amphibole veins with amphibole-rich alteration selvages occur locally. Grossularite garnet has been observed in veins and alteration selvages towards the western end of the system, close to the contact with granitic rocks.

Inclusion Petrography: The polished sections contained 2-25 mm quartz veins in calcite-biotite bearing host rock. The quartz has been highly deformed and recrystallised and thus many of the inclusions may have leaked or have been destroyed. There are however, abundant small, secondary inclusions(<1-20 mm) usually aligned parallel to the direction of shear. Many show evidence of necking and have inconsistent liquid/vapour ratios and hence data from these inclusions must be regarded as suspect. Types E and H were the most common inclusions in this sample but Types B, D and G were also observed.

Microthermometry: The microthermometric data indicates that most inclusions have depressed T_mCO_2 temperature thus indicating the presence of other volatiles. The CO_2 phases generally homogenise at between 20 and 27°C and estimates of CO_2 density generally vary from 0.67 to 0.77 g/cm^3, however, a few inclusions showed higher CO_2 densities of 0.88 and 0.95. Many of these inclusions decripitated at temperatures below 50°C but a few gave homogenisation temperatures between 222 and 310 °C.

Raman Spectroscopy: No gases were detected in Type B inclusions suggesting that they contain mainly water. Only CO_2 could be detected in Types E and H inclusions within the highly deformed quartz. However, some regions of non-deformed (later?) quartz contained inclusions with both CO_2 and CH_4 and perhaps some minor C_2H_6 and C_3H_8 as well.

MISSOURI

Production: 20.76 kg of gold from 1,674.6 t of ore at 12.4 g/t was produced between 1899 and 1912. Open pit mining between 1987 and 1988 is estimated to have yielded approximately 900 kg of gold from 300,000 t of ore at 3.0 g/t.

Host Rocks: Weakly plagioclase-phyric, low Mg series (Missouri) basalt.

Mineralised Structure: A 0.5 - 2 m wide fracture with abundant quartz veining and a small (<10m) dextral displacement. The overall character is predominantly brittle but it is associated with variable amounts of shearing as well. The fracture dips approximately 70°NE and breaks into several subparallel quartz veins at the eastern end of the open pit. These subsidiary quartz veins trend 345-355° and dip 45-70°NE, consistent with dextral displacement and NE-side-up movement.

Alteration: Quartz(-plagioclase)-biotite-carbonate-pyrite alteration assemblages are developed adjacent to quartz veining. Oriented biotite defines a weak but variable shear fabric. Pyrite occurs as coarse (up to 2 mm), idioblastic grains with small biotite-rich pressure shadows. Minor, late chlorite post-dates biotite and the shear fabric. The biotite-rich alteration assemblage is enveloped by a mildly chloritic outer alteration halo of a similar width.

Inclusion Petrography: The polished section contained a ca. 2 cm quartz-calcite vein in biotite-rich host rock. Many small inclusions (<1-20 μm) were observed in the quartz vein but none were observed in the calcite. The inclusions were irregular to rounded and appeared to be secondary with some showing evidence of necking. 100% vapour (Type G) inclusions were the most common with Types A and H inclusions also being observed.

Microthermometry: Measurements of T_mCO_2 indicated that some inclusions contained only CO_2 while others showed depression of T_mCO_2 indicating the presence of other volatiles. The CO_2 phases generally homogenised at temperatures between 12 and 30°C giving corresponding densities of 0.84 to 0.61 g/cm^3 (assuming a pure CO_2 phase) but a few inclusions with densities as high as 0.93 g/cm^3 were also observed.

Raman Spectroscopy: The Raman analyses confirmed the presence of 100% CO_2 inclusions but also found one microfracture which contained 100% CH_4 Type G inclusions. In the region surrounding this microfracture both gases were detected in fluid inclusions indicating possible mixing of CO_2-rich and CH_4-rich fluids.

BONNIE DOON

Production: 87.98 kg of gold from 2,937 t of ore at 29.9 g/t from 1897 to 1947.

Host Rock: Weakly porphyritic, low-Mg series (Missouri) basalt. There is also minor mineralization in the overlying ultramafic rocks of the Walter Williams Formation. Associated conformable sheared quartz-feldspar porphyry intrusives are probably not a significant host rock.

Mineralised Structure: Two sub-parallel shear zones up to 15 m wide and up to about 500 m long, trend 010-015°. They are probably conformable with enclosing basalts and may be partly localised by interflow sediments. The shear zones are commonly observed at basalt/porphyry contacts but also occur up to 10 m from the porphyry margins, separated by undeformed basalt. Quartz veining in the shear zone and the basalt is widespread and stockwork quartz veining occurs in the porphyries. Subsidiary structures occur to the west of the main structures and consist of :

- (i) a relatively brittle structure which dips 70°NW characterised by fewer, but larger, quartz veins than those in the main shears and,
- (ii) narrow (up to about 0.5 m) shear zones striking 340° and dipping about 80°E. These contain small (5-20 cm) quartz veins.

Alteration: The outer zone consists of weakly altered (minor disseminated carbonate, pyrrhotite, biotite) and little deformed metabasalt/amphibolite. An intermediate zone of recrystallised amphibolite occurs marginal to the inner alteration zone. This zone contains minor quartz, carbonate and disseminated pyrrhotite. Amphibole (hornblende?) in these foliated rocks is coarser grained, and possibly more aboundant. Although oriented amphiboles produce a fabric of variable intensity, amphiboles oriented at large angles to the dominant fabric are common. An inner zone of biotite-plagioclase-carbonate-pyrite alteration is associated with quartz-carbonate-pyrite (-minor amphibole) veining. A narrow (2 mm) selvage of granoblastic plagioclase (albite?) and minor carbonate occurs adjacent to some of these veins. Oriented biotite defines a weak but variable planar fabric. Minor, unoriented, subhedral amphibole (hornblende?) is locally concentrated in foliation-parallel bands, and more irregular domains of biotite, and appears to overprint the biotite fabric. Tremolite-rich rocks in which minor albite occurs interstitially to unoriented prismatic to acicular tremolite-actinolite may be altered porphyry.

Inclusion Petrography: The polished section contained quartz-calcite veins in biotite rich host rock. Abundant fluid inclusions (<1-20 μm) were observed in the quartz but none were observed in the

calcite. The inclusions are irregular to rounded often with evidence of necking and appear to be pseudosecondary or secondary. Most inclusions contained 100% vapour (Type G) but Type E and some apparently late Type B inclusions were also observed.

Microthermometry: The data showed T_mCO_2 values indicating inclusions with pure CO_2 and others that also contained another volatile species. Clathrate melting temperatures indicate salinities around 4-5 eq. Wt% NaCl. The CO_2 phases homogenised at temperatures between 19 and 31°C giving corresponding densities of 0.79-0.52 g/cm^3. Two inclusions homogenised at around 136°C and one Type B inclusion homogenised at 252°C but most inclusions decripitated at temperatures above 200°C.

Raman spectrometry: The Raman analyses of the vapour phases in a small number of these inclusions showed that there were 3 categories:

- (i) Inclusions with approx. equal amounts of CO_2 and CH_4
- (ii) CO_2 rich inclusions with approx. 6 mol.% CH_4, and
- (iii) Late secondaries (Type B) containing no detectable gases in the vapour phase

---

SUNDAY GIFT

Production: 43.8 kg of gold from 817.4 t of ore at 53.6 g/t from 1897 to 1913.

Host Rocks: Fine grained amphibolite (after low-Mg series basalt).

Mineralised Structure: Several 190°-trending, subvertical shear zones, with quartz veins up to 0.3 m wide.

Alteration: An outer alteration halo consisting of foliation-controlled biotisation and silicification (with minor epidote, calcite and sulfides) envelopes and an inner, massive to banded quartz-amphibole assemblage. The inner assemblage contains variable but mostly minor chlorite, carbonate, plagioclase, titanite and pyrrhotite. Amphibole in both assemblages is randomly orientated and overprints the metasomatic shear.

Inclusion Petrography: The polished section contained quartz-calcite veins in amphibole-biotite host rock. A few fluid inclusions (<1-20 μm) were observed in the quartz but extensive recrystallisation has destroyed most of them. None were observed in the calcite. The inclusions appeared to be pseudosecondary and were rounded to negative crystal in shape. They were mostly 100% vapour (Type G) but some Type H inclusions were also observed.

Microthermometry: The data showed depressed T_mCO_2 values indicating that methane and/or other gases were probably present. The CO_2 phases homogenised at temperatures between 18 and 31°C corresponding to densities between 0.8 and 0.54 g/cm^3. This large range suggests that some inclusions have leaked or changed volume and so the data must be regarded as suspect.

GOODENOUGH

Production: Historic production of 201.89 kg of gold from 4,543 t of ore at 44.4 g/t (1897- 1940). Recent production of 62.85 kg of gold from 8,478 t of ore at 7.2 g/t (1981-1984).

Host Rocks: Mainly quartz-plagioclase-biotite schist (probably after granitoid-derived sedimentary rocks) and minor mineralisation in fine grained amphibolite. An intrusive quartz-plagioclase-biotite porphyry cuts across the mineralised structure and hosts minor mineralisation in deformed marginal zones.

Mineralised Structure: Approximately east-west trending shear zone which dips 25-35°S, located on the contact between felsic schist (footwall) and mafic rocks (hanging wall). Mineralisation is associated with a 1-2 m thick zone of banded quartz-sulfide ± biotite rock within the broader zone of shearing. Foliation parallel quartz veins are commonly stretched, boudinaged, ruptured and otherwise deformed. Late brecciation and veining of the banded shear structure is a relatively minor feature.

Alteration: Pyrite occurs as coarse, irregular masses up to several centimetres across and is locally semimassive. Less intensely altered metasedimentary rocks contain minor amounts of ilmenite, pyrrhotite and chalcopyrite as elongate disseminations in biotite-rich or sphene-rich shear planes. These minerals are partly replaced by pyrite, which together with small amounts of carbonate (calcite) and muscovite, increase in abundance towards the centre of the mineralised shear. Spatial associations suggest pyrite, calcite and muscovite were introduced during the formation of early quartz veins that are now boudinaged and recrystallised. Veins and breccia containing coarse muscovite (commonly fuchsite), carbonate and pyrrhotite, with minor pyrite and pentlandite, formed during late brittle deformation of sheared sedimentary rocks adjacent to the banded quartz-pyrite rock. Unoriented muscovite porphyroblasts (≤ 0.2 mm) overgrow the foliation in weakly altered rocks adjacent to the veins, and contain irregular inclusions of quartz and plagioclase. The amount of muscovite porphyroblasts and associated carbonate increase steadily towards the veins and zones of brecciation, suggesting formation during this later phase of deformation. Altered mafic rocks are banded quartz-amphibole-plagioclase rocks with minor chlorite, carbonate, sericite, pyrite and sphene. Quartz is mostly variably recrystallised, foliation-parallel vein material. Amphibole (hornblende?) is variably oriented but unoriented amphibole appears to have preferentially replaced chlorite-rich bands and biotite-rich bands. Relic chlorite displays anomalous brown interference colours, and biotite is mostly replaced by sericite. A later variety of chlorite also occurs as spaced, through-going shear planes.

Inclusion Petrography: The polished section contains quartz veins in sulfide rich host rock. The quartz has been strongly deformed and recrystallised but contains abundant small inclusions (<1-20 μm). All inclusions contain 100% vapour (Type G) and are secondary. They are irregular to rounded and some show signs of decrepitation. Thus data from these inclusions must be regarded as suspect.

Microthermometry: The microthermometric data shows depression of T_mCO_2 values indicating the presence of other volatiles. The CO_2 phases homogenised over a wide range of temperatures varying from -21 to 14°C indicating density variations from 1.04 to 0.83 g/cm^3.

Raman Spectroscopy: Raman analyses from these inclusions showed varying proportions of CO_2 and CH_4 were present. The inclusions appeared to be either CO_2 dominant or CH_4 dominant suggesting that there are either two fluids or a marked change in oxidation state of the fluid over time.

YUNDAGA

Production: 8,757.89 kg of gold from 507,824.9 t of ore at 17.2 g/t from 1897 till 1935. Recent exploration has outlined ore reserves of 1,293 kg of gold from 460,000 t at 2.81 g/t.

Host Rocks: Fine to coarse grained felsic, granodiorite-derived arkosic sediments, including conglomerate containing granodiorite clasts up to about 10 cm. Ultramafic schist and mafic sediments occur on the footwall of the mineralised structure. All rock types occur as tectonic slices within the Boorara—Menzies Shear Zone.

Mineralised Structure: NNW-striking shear zones dip about 60°W within pervasively foliated sediments and are broadly conformable with the structural grain of the regional shear zone. Ore shoots consist of banded, "cherty"-looking rocks, up to about 1 m thick, in which the foliation is defined by mineral banding and oriented phyllosilicate minerals. The main orebody (Princess May)

consists of several ore shoots and is approximately 400 m in strike length at the surface and plunges at about 35°S to a depth of 250 m.

Alteration: Mineralised shears within sediments are banded quartz-sericite(± siderite)-pyrite schist. Quartz-rich bands may result from foliation-controlled silification, or from deformation and recrystallisation of earlier formed quartz veins. Pyrite occurs as foliation-parallel trails of anhedral, slightly elongate disseminations and discontinuous veinlets, indicating recrystallisation during ductile deformation. Minor idioblastic arsenopyrite occurs locally, adjacent to some late, relatively undeformed, foliation-parallel quartz veins. Ultramafic rocks are altered to talc-chlorite-carbonate (ferroan dolomite) schist in which up to about 30% unoriented tremolite prisms overgrow the chloritic shear fabric. Disseminated rutile and zircon occur in the chloritic bands. More strongly deformed and altered shear zones within ultramafic rocks are recrystallised to a banded quartz-tremolite ± biotite rock. The tremolite is coarse (up to 1 cm) and prismatic except when adjacent to quartz-rich bands where it adopts a finer grained, fibrous to acicular habit. Biotite and tremolite are unoriented and represent a post-deformation, metamorphically recrystallised metasomatic assemblage. Ultramafic hosted mineralisation is associated with disseminated pyrrhotite (with some minor pyrite and chalcopyrite) which occurs as foliation-parallel trails of slightly elongate, anhedral disseminations.

Inclusion Petrography: The polished section contained 5-15 mm quartz-calcite veins in strongly sheared rock. However, small, undeformed crystals (<20 μm) of brown or green hydrothermal biotite also occur in the quartz-calcite veins. The quartz contained abundant inclusions (<1-30 μm) but none were observed in the calcite. The inclusions are irregular to rounded with some showing evidence of necking and are pseudosecondary to secondary. Types A, B, C and G were observed. The solid phase in Type C inclusions was identified as calcite by Raman spectroscopy. Type A inclusions appear to have consistent liquid/vapour ratios in individual microfractures but variable L/V ratios were observed overall.

Microthermometry: The data shows significant depression of T_mCO_2 values indicating the presence of other volatiles, most probably CH_4. The CO_2 phases homogenised over a wide range of temperatures from -14 to 22°C giving density variations from 1.01 to 0.75 g/cm^3. A few inclusions showed a possible clathrate melting at around -1.0°C which would indicate a moderate salinity fluid however these were very hard to observe and if it was ice melting then it would be a low salinity fluid. Some Type B inclusions homogenised at temperatures between 124 and 252°C but these could be late secondaries. Most inclusions decrepitated at temperatures above 300°C with the exception of one Type A inclusion which homogenised at 409°C.

LADY HARRIET

Production: Exact production is unknown. Woodward (1906) indicates 110.81 kg of gold from 3,493 t of ore at 31.7 g/t to 1905.

Host Rocks: Fine grained felsic to mafic sedimentary rocks (and minor interleaved amphibolite?) within the Boorara–Menzies Shear Zone.

Mineralised Structure: Two shear zones, mineralised over a strike length of about 100 m at the surface, and broadly conformable with the structural fabric of the regional shear zone. Both shear zones strike 155° and dip about 70°E and are 1-3 m wide. They contain numerous quartz ± sulfide veins up to 20 cm wide, mostly conformable with the shear fabric. Woodward (1906) describes the orebody as consisting of four pipes which pinch out at about 60 m depth.

Alteration: Mafic sediments are altered to a banded rock containing a complex assemblage dominated by calcic plagioclase, chlorite and biotite. Other minerals include quartz, garnet, chloritoid,

calcic amphibole, and opaque minerals. Mineral banding on the scale of <1-10 mm is defined predominantly by modal variation of plagioclase, quartz, and phyllosilicate mineral assemblages. Calcic plagioclase occurs as a mosaic of slightly elongate, lens-shaped grains outlined by anastomosing biotite-rich seams and as zoned snow-flake shaped porphyroblasts. Biotite and more particularly chlorite are strongly orientated within phyllosilicate-rich bands. Almandine-rich garnet occurs in both chloritic bands and plagioclase-biotite bands, but inclusion trails in garnet from chloritic bands are commonly rotated while those in plagioclase-biotite bands are continuous with the external foliation. This is interpreted to indicate that the chloritic bands are retrograde shear planes along which movement occurred after crystallisation of garnet.

Iron-rich chloritoid occurs as unorientated prisms in biotite-chlorite bands and plagioclase-biotite bands. Inclusion trails of plagioclase, quartz and carbonate are generally continuous with the external foliation. Calcic amphibole (hornblende) occurs as unoriented prisms in biotite-chlorite bands and plagioclase-biotite bands. Up to several percent ilmenite and pyrrhotite with variable pyrite and minor chalcopyrite occur as anhedral disseminations recrystallised in the plane of the foliation. Minor arsenopyrite was also observed but this is coarser grained and displays less evidence of recrystallisation, suggesting later growth.

Inclusion Petrography: The polished section contained a couple of quartz veins (<1-3 mm) in chlorite/amphibole-rich rocks with garnet porphyroblasts. Evidence was observed for the replacement of deformed biotites with finer grained chlorite. Abundant fluid inclusions (<1-20 μm) were observed in the quartz veins but the garnet porphyroblasts contained mostly solid inclusions. The inclusions were irregular to rounded and secondary. Types B, C (rare), G and H were observed. Most inclusions contained only a carbonic phase and those with an aqueous phase also showed consistent liquid/vapour ratios.

Microthermometry: The microthermometric data showed depressed T_mCO_2 values indicating that methane (or nitrogen) is probably present. The CO_2 phases generally homogenised at temperatures between 18 and 22° C with corresponding densities of 0.79 to 0.75 g/cm^3. Final ice melting temperatures indicated that type B inclusions had low to moderate salinity. Type B inclusions also homogenised at temperatures between 186 and 253°C.

LADY SHENTON

Production: 5,836.9 kg of gold from 171,199 t of ore at 34.1 g/t (1897-1942).

Host Rocks: Predominantly fine to coarse grained amphibolite within the Boorara—Menzies Shear Zone, but also probably some production from coarse grained, arkosic metasedimentary rocks.

Mineralised Structures: A 160°-trending shear zone dips approximately 45°W and is subconformable with the structural grain of the enclosing regional shear zone. The shear zone is mostly within mafic rocks but merges with granitoid-derived metasediments at about 350 m depth. Lenticular, pipe-like quartz 'reefs' plunge about 35°S and merge towards the surface to form a 200-300 m long ore zone. The quartz 'reefs' pinch out down plunge at about 120 m. Ore shoots are offset by east-west and north-dipping faults ('cross courses'), but ore shoots are also *en echelon* in character, being boudinaged rather than offset.

Alteration: Mafic rocks display foliation-controlled biotitisation. Increasing intensity of alteration produces a strongly banded, 'cherty' quartz-biotite-calcic plagioclase rock. Quartz-rich bands probably represent foliation-controlled silicification as well as recrystallised foliation-parallel quartz veins. Minor components include calcic amphibole, carbonate (calcite), and opaques. Unoriented calcic amphibole overgrows the shear fabric and is particularly well developed in and adjacent to foliation-parallel carbonate-rich bands. The predominant sulfide minerals are pyrrhotite and

arsenopyrite with minor pyrite and chalcopyrite, largely concentrated in biotite-rich, quartz-poor bands. Woodward (1906) records the presence of galena and sphalerite. Pyrrhotite occurs as fine disseminations which form foliation-parallel trails, and as coarser, angular disseminations interstitial to unoriented biotite. These features suggest that the pyrrhotite was introduced during the early stages of deformation and recrystallised with biotite. Arsenopyrite and pyrite form coarser disseminations up to about 0.5 mm and tending toward idioblastic form suggesting relatively late growth. Minor retrograde chloritisation occurs locally, and is probably related to late cross-cutting shears. Arkosic metasediments are altered to pyritic quartz-sericite(± carbonate) schist.

Inclusion Petrography: The polished section contained 5-10 mm quartz veins in a carbonate-rich, strongly sheared host rock. Abundant very small (<1-10 μm) inclusions were observed in the quartz. The inclusions are rounded to negative crystal in shape and secondary. Only Type G and Type H inclusions were observed.

Microthermometry: The microthermometric data show depressed T_mCO_2 values indicating that other gases (e.g. CH_4 or N_2) may also be present. The CO_2 phases generally homogenised between 12 and 24° C corresponding to densities between 0.84 and 0.73 g/cm^3. One inclusion gave a density of 0.88 g/cm^3.

Raman Spectrometry: The Raman analyses confirmed the presence of both CO_2 and CH_4 in the carbonic phases of these inclusions. The methane content was observed to vary from about 10% up to 53% suggesting that mixing of a CO_2 rich and a CH_4 rich fluid may have occurred.

ASPACIA

Production: Exact figures are not known but production attributed to the Menzies Mining and Exploration Corp. Ltd. is 963.33 kg of gold from 25,993 t of ore at 37.1 g/t which may include some production from Lady Shenton as well.

Host Rocks: Fine to coarse grained amphibolite in the Boorara–Menzies Shear Zone.

Mineralised Structure: A broad zone (20-50 m) of sheared mafic rocks trending 140° and dipping 50-80°SW. Mineralisation is associated with broadly conformable quartz bands (veins?), 0.1 to 1.0 m, within the shear zones and locally with brecciated sections.

Alteration: Foliation-controlled biotisation becomes increasingly intense towards a quartz-biotite-plagioclase assemblage in the shear centres. Late metamorphic amphibole overprints the shear fabric in biotised zones. Disseminated pyrrhotite and pyrite increases in abundance towards the inner zone of alteration. Coarse, anhedral pyrrhotite interstitial to unoriented amphibole suggests static recrystallisation of the sulfide with calcic amphibole in some bands. Sphalerite is also abundant in some quartz-rich bands.

Inclusion Petrography: The polished section contained a quartz vein (~20mm) in banded sphalerite/sulfide host rock. Abundant small (<1-20 μm) inclusions were observed in the quartz. The inclusions appear pseudosecondary or secondary and are irregular to rounded. Only monophase (Type G) inclusions were observed.

Microthermometry: Microthermometric data showed depressed T_mCO_2 values indicating that methane or nitrogen may be present. Relatively low Th CO_2 values were recorded indicating densities between 0.89 and 1.01 g/cm^3.

Gold Deposits Associated with Alteration Assemblage 4

ST ALBANS

Production: 34.8 kg of gold from 714.8 t of ore at 48.7 g/t between 1898 and 1908.

Host Rocks: Mainly fine grained amphibolite (after mafic volcanics?), interleaved with minor talc-chlorite-tremolite schist (after komatiitic volcanics?) within the Menzies Shear Zone. An associated garnetiferous (spessartine) albitite is unmineralised.

Mineralised Structures: Most of the gold was produced from ENE-trending quartz veins which dip about 45°S. The veins are up to about 100 m long at the surface and 0.1 to 2 m wide. There is little or no shearing adjacent to the veins. East-west quartz veins are associated with (and probably postdate?) conformable zones of high strain in the host rock amphibolite and schist. These zones of intense shearing (up to 1 m wide) strike 150° and dip 50-60°SW and probably also carry some mineralisation.

Alteration: Conformable shear zones are associated with calc-silicate alteration of amphibolite. Foliation-parallel bands of diopside (± grossularite-rich garnet) and minor quartz and calcite replace calcic amphibole and calcic plagioclase. Epidote (± quartz) occurs in variable amounts, up to almost 50% locally. It appears to be replaced by the calc-silicate assemblage in some bands, but other foliation-parallel bands display little evidence of recrystallisation and may post-date growth of calc-silicate minerals. Trace disseminated rutile in amphibolite is replaced by granular sphene in calc-silicate bands. Foliation-parallel bands or seams of biotite are subordinate with respect to calc-silicate alteration. Minor associated tremolite-chlorite schist (± talc) may represent recrystallised (and altered?) ultramafic rock. Foliation is defined by oriented chlorite and tremolite needles or prisms. However, unoriented tremolite prisms are also common. Trace amounts of disseminated rutile form foliation-parallel trails. However, there is little or no apparent alteration adjacent to the mineralised east-west quartz veins.

Inclusion Petrography: The host rocks contain garnet, epidote, diopside, quartz and calcite. Sample 98222 contained mostly solid inclusions but a few large inclusions (up to 50 μm) were observed in the epidote. Sample 98222A contained fairly small inclusions (<1-10 μm) in the garnet with a few trails of small inclusions also being observed in the calcite. The inclusions are rounded to negative crystal in shape and appear pseudosecondary or secondary. Types A, B and C were observed with consistent liquid/vapour ratios being observed in sample 98222A.

Microthermometry: No CO_2 could be observed during the microthermometry. The carbonic phase appears to contain only methane which homogenised by critical behaviour. Thus homogenisation was difficult to observe but one inclusion showed $l+v(v)$ homogenisation of the carbonic phase just a few degrees below the CH_4 critical point (-82°C) while another exhibited $l+v(v)$ homogenisation of the carbonic phase at -112.7°C. These temperatures indicate that the density of the carbonic phase is between 0.05 and 0.4 $gm.cm^{-3}$. Some irregular shaped, secondaries in epidote contained up to 5 daughter crystals. A few inclusions showed low $T_m$ice values, indicating the presence of divalent or trivalent cations in solution. The vapour phase in these inclusions disappeared at temperatures between 247 and 361°C but the solids in Type Cs did not dissolve at temperatures up to 400°C.

Raman Spectrometry: The Raman microprobe analyses confirmed the microthermometric observations with only methane being detected in the vapour phase for all inclusions in both epidote and quartz. Raman spectra were also recorded from some of the solid phases in the Type C inclusions but only calcite could be identified. The other solids are likely to be ionic chloride salts.

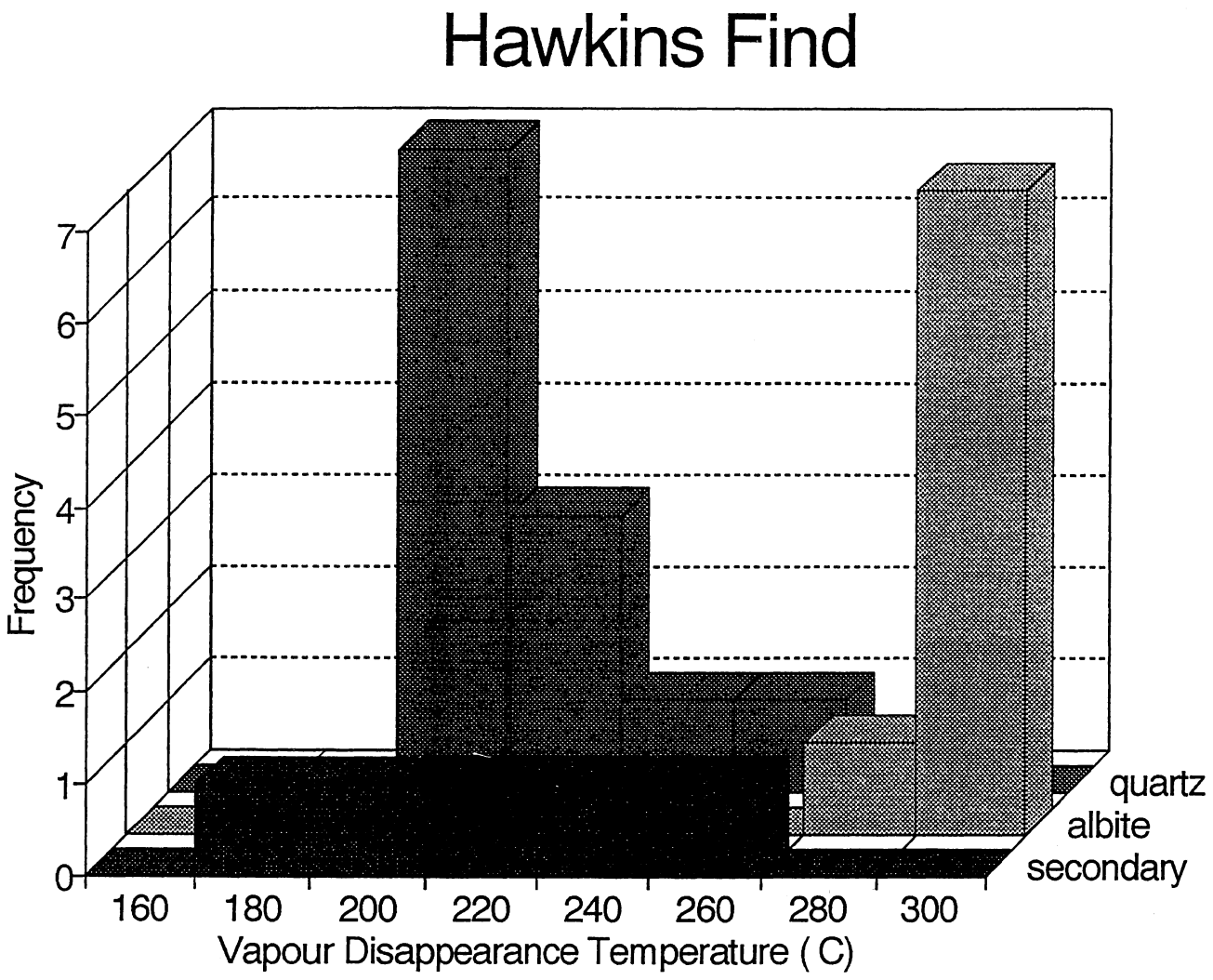

Figure 4. Vapour disappearance temperatures for inclusions in albite and quartz, and secondary inclusions from Hawkins Find.

DISCUSSION

To ascertain whether the fluid inclusion reconnaissance reflects the increasing temperature and variations in X_{CO2} predicted in Table 1, a comparison of the data for the various metamorphic and metasomatic assemblages associated with mineralisation in the mafic rocks has been made.

Figure 3 shows a histogram of vapour disappearance temperatures for assemblages 1, 3 and 4. Assemblage 2 contained only 100% CO_2 inclusions (see below). Note that some inclusions contained solids which did not dissolve on heating well above the homogenisation temperature of the other phases and hence, may be accidentally trapped solids. Figure 3 also shows evidence for a bimodal distribution of homogenisation temperatures in assemblage 1. All data for assemblage 1 comes from Hawkins Find as an aqueous phase was not observed in the inclusions from Binduli. The data for Hawkins Find is shown in more detail in Figure 4. This figure shows that the more CO_2 rich inclusions in albite have higher homogenisation temperatures around 300°C while those in quartz have a mode at 200°C. Although only a few secondaries were examined their temperatures appear to cover a similar range to that of quartz. This suggests that the quartz is relatively later than albite and is consistent with the mineral paragenesis which shows albite forming on the margins of vughs which have central quartz cores.

All data for assemblage 2 comes from the Goongarrie deposits. However, once again no aqueous phase could be observed in the carbonic inclusions and all inclusions gave CO_2 homogenisation

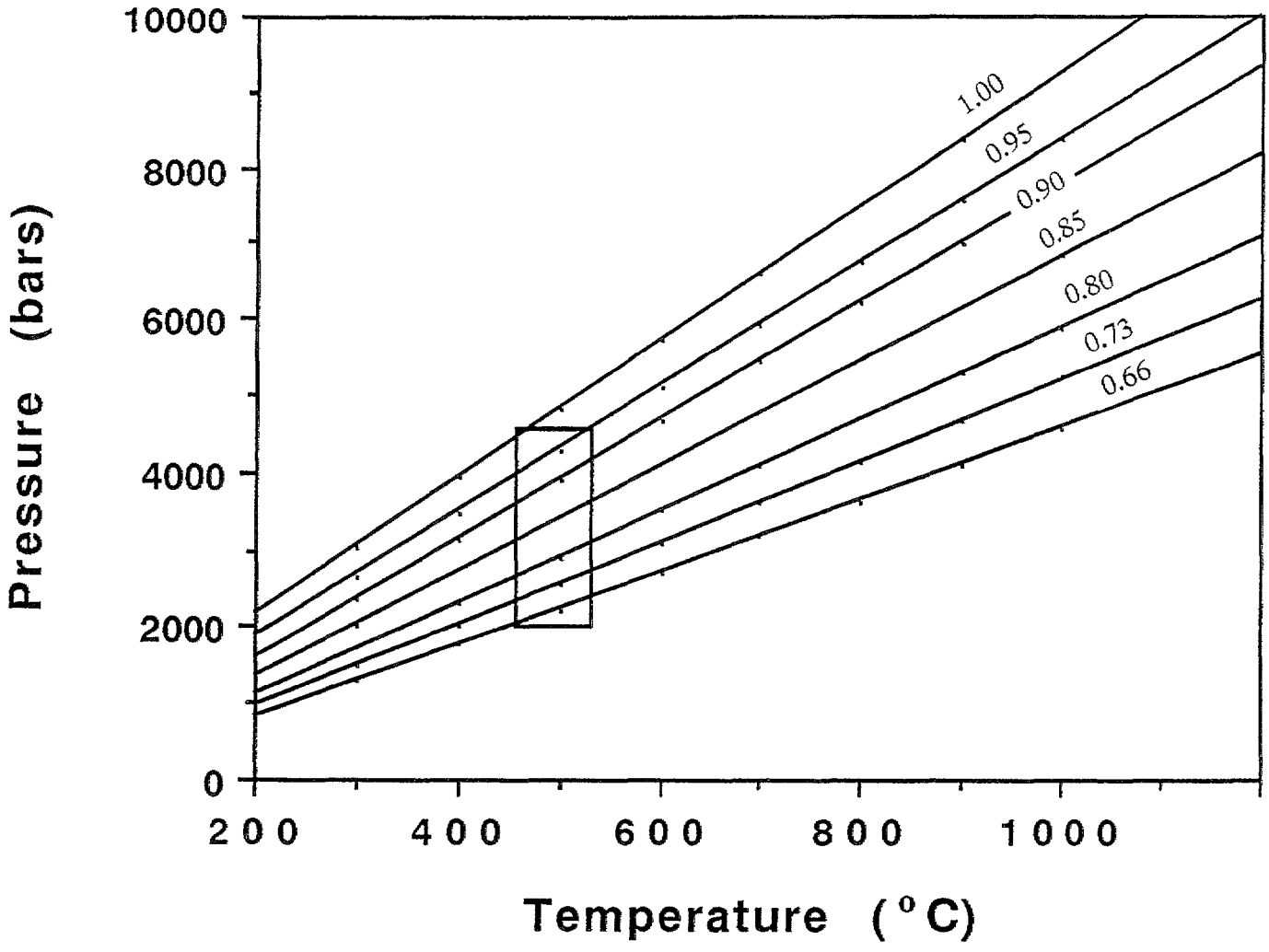

Figure 5. P-T diagram showing isochores for the system CO_2-H_2O-NaCl (6 wt %) as calculated using the procedure of Brown and Lamb (1989). The box represents the expected range in pressure for inclusions with these densities trapped at temperatures around 500°C.

temperatures between 16 and 21°C. The observation of carbonic gas-rich inclusions with little or no observable aqueous phase has previously been reported from Paringa, Mt Charlotte, Lancefield, Ora Banda and Water Tank Hill in the Yilgarn Block (Ho, 1987) and from the McIntyre-Hollinger gold deposit in Canadian Shield (Smith *et al.*, 1984).

Assemblage 3 includes data from 9 of the 13 deposits examined in this study and shows a greater variation in homogenisation temperatures than that observed for assemblages 1 and 4 (see Figure 3). However, most deposits have homogenisation temperatures within the range 160 to 360°C with an average of 236°C and only one inclusion was observed to homogenise above 400°C. Thus, these temperatures are somewhat lower than the approximately 500°C temperature predicted from the metasomatic mineral assemblages and suggests that a pressure correction needs to be applied to the data. Calculations based on the equations of Brown and Lamb (1989) indicate that these inclusions have bulk densities between about 1.00 and 0.66 gm.cm^{-3} with an average value of 0.88 gm.cm^{-3}. If a trapping temperature of approximately 500°C is assumed, then Figure 5 indicates that these inclusions may have formed at pressures between about 2.0 and 4.5 kbar.

Assemblage 4 shows generally higher homogenisation temperatures with a mode near 340°C. This is well below the temperature predicted by the metamorphic mineral assemblage and once again

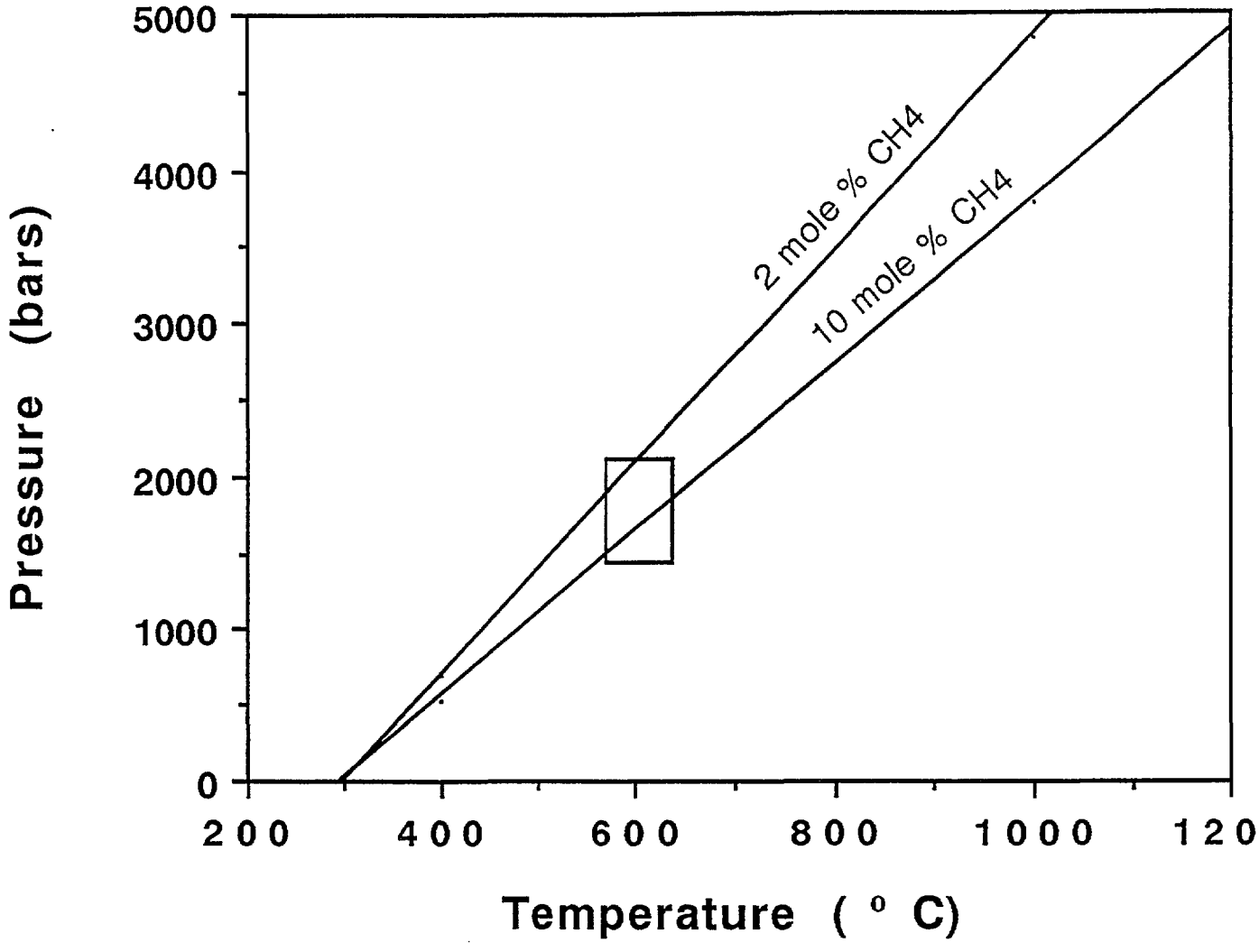

Figure 6. P-T diagram showing isochores in the CH_4-H_2O system (modified from Thomas and Spooner, 1988). The box represents the expected range in pressure for inclusions trapped at temperatures around 600°C. Note that inclusions with higher methane contents would form at even lower pressures.

suggests that a pressure correction is required. Only inclusions from the St. Albans deposit were examined in this study but Types A, B and C inclusions were observed in epidote, garnet and quartz. Raman microprobe analysis showed that assemblage 4 contained only methane in the vapour phase with CO_2 being below detection limits. Calculations based on the method of Thomas and Spooner (1988) indicate that the inclusions would have been trapped at pressures approaching 2 kbar if they were formed around 600°C (see Figure 6). This is consistent with the proposal that the high grade metamorphism results from the intrusion of late syntectonic granites.

Final CO_2 melting temperatures for assemblages 1-3 are shown in Figure 7. Data from the Binduli deposit (Assemblage 1) shows that these inclusions contain CO_2 as the only carbonic component. Similar results have been reported for the Golden Mile, Paddington, Lady Bountiful and Ora Banda deposits which also belong to this category (Ho *et al.*, 1990). Raman microprobe analyses of inclusions from Hawkins Find (see Figure 8) indicates that the inclusions in quartz have complicated mixtures of CO_2, N_2 and CH_4 with most containing mainly $CH_4 \pm N_2$. Methane has also been reported from the Stage 3 mineralisation at Mount Charlotte but data on the trapping temperature of these inclusions is not yet available.

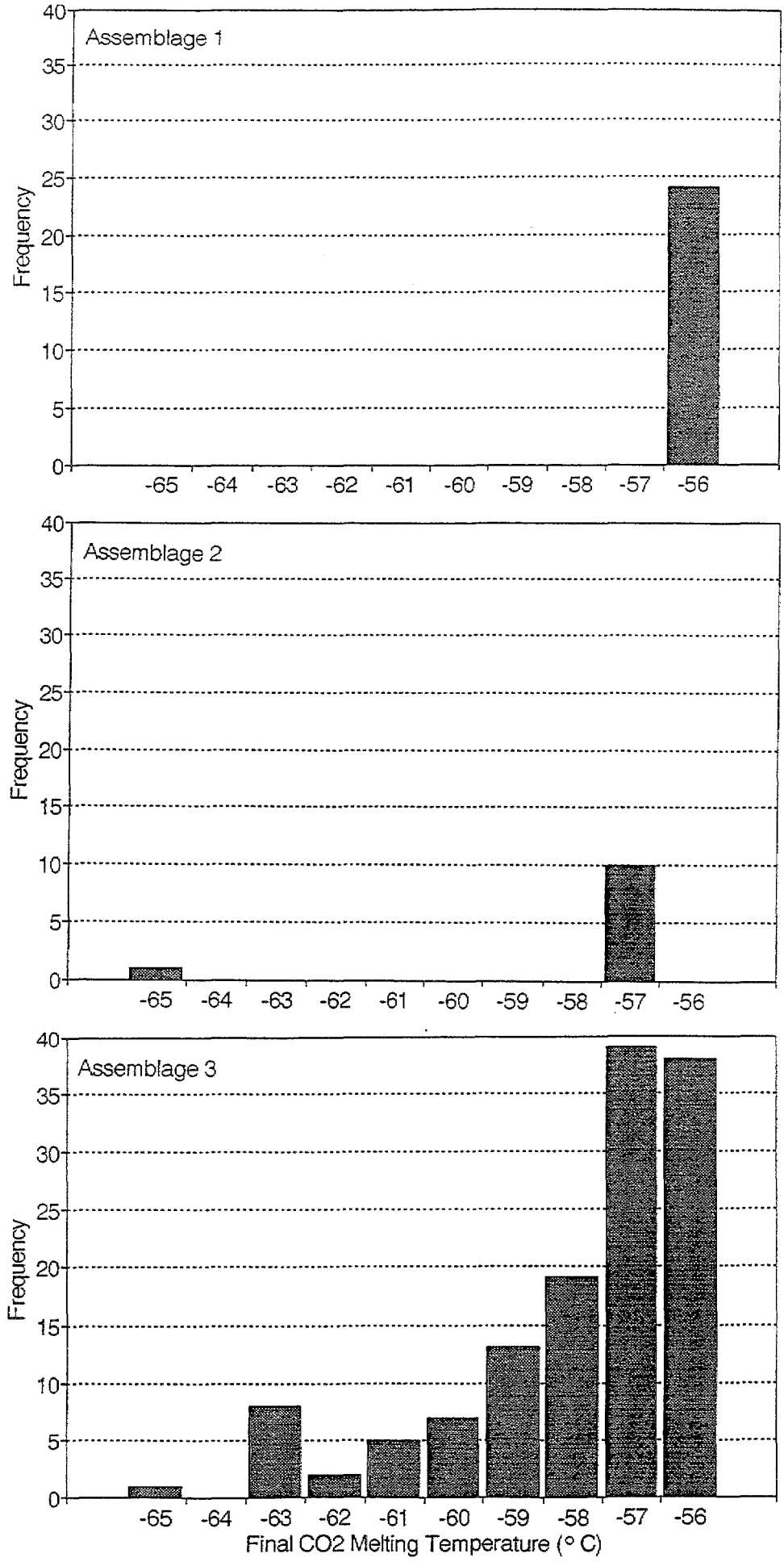

Figure 7. Final melting temperatures for solid CO_2 in assemblages 1,2 and 3 (cf. Table 1).

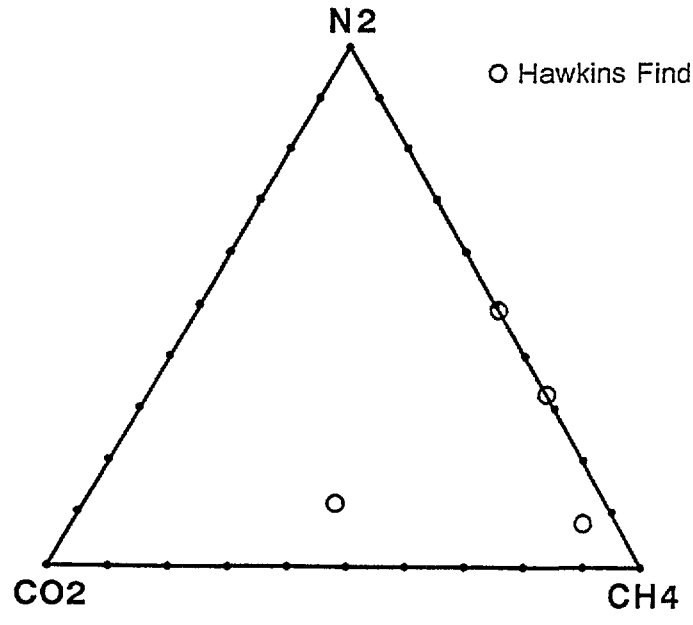

Assemblage 1

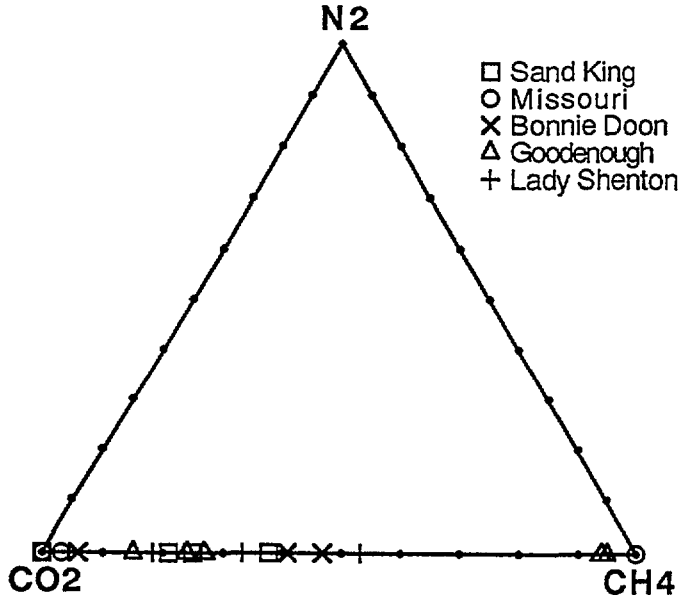

Assemblage 3

Figure 8. A plot of Raman microprobe analyses of the vapour phase in inclusions from selected deposits of Assemblage 1 and Assemblage 3.

Most inclusions from Assemblage 2 show only a slight depression of the CO_2 final melting temperature indicating that carbonic phase contains mostly CO_2 which was confirmed by Raman microprobe analyses. There was however, one inclusion with a CO_2 final melting temperature of -66.1°C suggesting a significant quantity of another gas (probably CH_4 or N_2) in this inclusion. Only CO_2 has been detected in the carbonic phase of inclusions from Victory-Defiance and the Hunt mines (Ho *et al.*, 1990) which also belong to Assemblage 2.

Although the majority of inclusions from deposits in Assemblage 3 have CO_2 final melting temperatures indicating nearly pure CO_2 there is a considerable tail on the low temperature side as shown in Figure 7. The Raman microprobe analyses of the vapour phase of inclusions from selected deposits within assemblage 3 are also presented in Figure 7. They show that the carbonic phases of these inclusions contain only CO_2 and CH_4 or mixtures of the two.

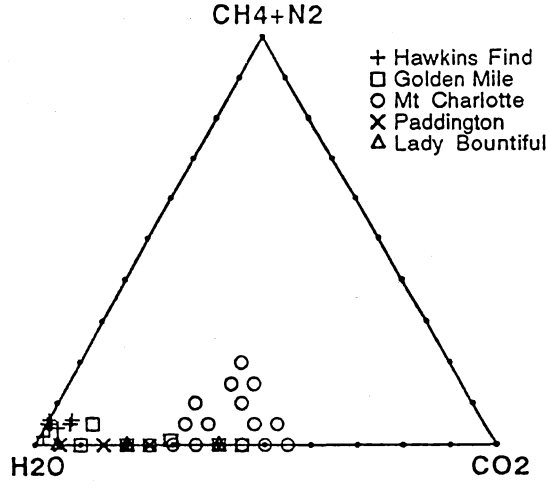

Assemblage 1

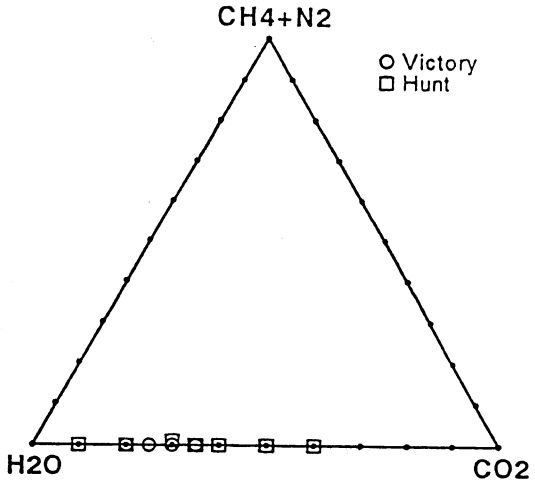

Assemblage 2

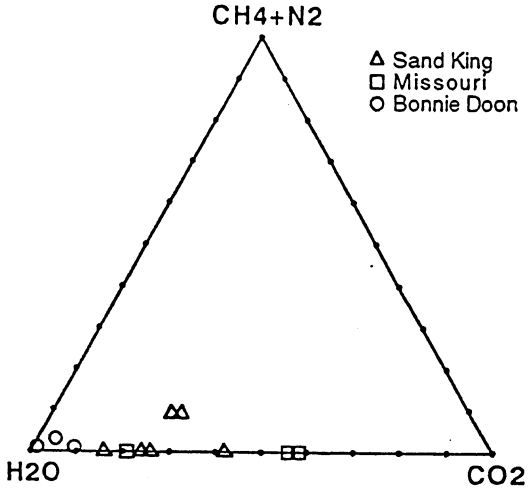

Assemblage 3

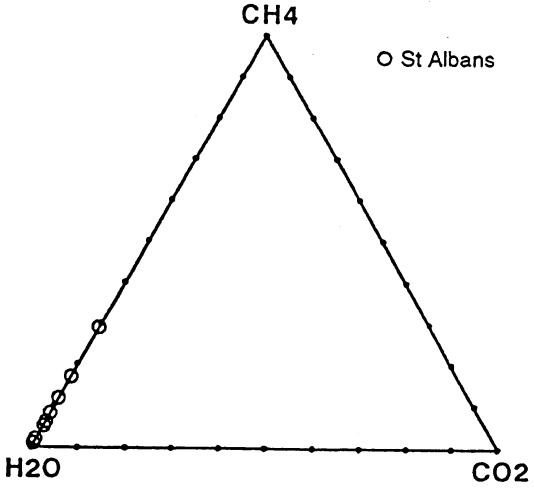

Assemblage 4

Figure 9. Plots of the bulk fluid composition in weight percent for deposits in Assemblages 1 to 4 which contained inclusions with aqueous and carbonic phases. Data for the Golden Mile, Mt Charlotte, Paddington, Lady Bountiful, Victory-Defiance and Hunt are taken from Ho *et al.* (1990).

Ho *et al.*, (1990) have studied fluid inclusions from deposits up to lower amphibolite metamorphic grade in the Yilgarn Block and have concluded that the ore forming fluids for these deposits typically contain between 10 and 45 weight percent CO_2. However, it is interesting to note that CH_4 ($\pm N_2$) was detected in assemblages 1-4 in the Menzies—Kamblada area and no CO_2 at all was detected in the inclusions from St. Albans (Assemblage 4). CH_4-rich fluids have been identified at Lancefield but the presence of CH_4 has only been previously noted in a few other deposits (e.g. the Golden Mile, and Mount Charlotte).

The bulk compositions of the fluids as determined from analysis of the fluid inclusions for assemblages 1-4 are shown in Figure 9. As shown above, only carbonic fluids were observed in a large number of samples examined in this study. Thus, bulk fluid compositions could only be estimated from those deposits where both aqueous and carbonic inclusions were observed. Due to the scarcity of aqueous inclusions in samples from Assemblages 1 and 2, data from Ho *et al.*, 1990 has been used to supplement the diagram.

Although there is considerable variation in fluid compositions, Figure 9 shows that assemblages 1 to 3 all contain significant amounts of CO_2 (up to 60 wt %). Fluids from Assemblage 1 also contain CH_4 in varying proportions up to 20 weight percent. The presence of CH_4-rich fluids in the low metamorphic grade of Assemblage 1 is consistent with other studies of variations of fluid inclusion composition with metamorphic grade. A "geotraverse" across a series of metamorphic zones in the Central Alps of Switzerland has been summarized by Frey *et al.*, 1980. Hydrocarbon and CH_4-rich fluids were observed for assemblages formed at up to 300°C, H_2O became dominant at temperatures around 450°C and CO_2 was the dominant species in high grade metamorphic rocks. The change from major CH_4 at low temperatures to major H_2O as temperature increases has been attributed to C-O-H equilibria involving graphite (Eugster and Skippen, 1967).

However, the trend from hydrocarbon-rich fluids at low metamorphic grades to CO_2-rich fluids at high metamorphic grades is not apparent in Figure 9. With the exception of Assemblage 4, all assemblages contain some inclusions with CO_2 concentrations well above the estimated average value of 25 to 30 wt % CO_2 (Ho *et al.*, 1990). In fact, as stated earlier, inclusions containing only a carbonic phase (i.e. Types G and H) are very abundant and are the only inclusions observed at some deposits. Similar carbonic fluid inclusions have recently also been observed in auriferous veins in the Zuru schist belt of northwestern Nigeria (Garba and Akande, 1992). The Nigerian schist belts have many features in common to greenstone belts and the latter authors suggest that phase separation led to the loss of H_2O and the selective entrapment of CO_2 in the fluid inclusions. Thus, it seems likely, that phase separation (boiling) has also occurred in the Menzies—Kambalda region with the subsequent loss of the H_2O-rich fluid phase.

The absence of CO_2 in the fluids from Assemblage 4 may indicate that it formed at very low oxidation conditions which converted all carbonic species to CH_4 but only a small amount of data has been collected from this deposit and further work to determine whether or not CO_2-bearing fluids are present in this deposit. A possible explanation for the high levels of CH_4 observed in the Menzies—Kambalda area is that the fluids trapped in the inclusions represent a mixture of two fluids, one being the CO_2-rich (ore-bearing?) fluid and the other derived from the wall rock ($CH_4 >> CO_2$). The wallrock fluid may have been formed as a result of metamorphic dehydration reactions at low oxygen fugacities in the carbonaceous black shales which are common as interflow sedimentary units in the greenstones of this area. A C-O-H fluid phase in equilibrium with graphite at QFM or lower fO_2 at temperatures between 400 and 600°C would contain significant CH_4, especially at higher pressures (French, 1966). For example at 500°C, 2 kbar and QFM-2, fluids on the graphite boundary consist of ~85 mole % CH_4 and ~15 mole % H_2O (Holloway, 1981). This is consistent with the observation of inclusions containing 100% CH_4 vapour in quartz from Missouri. Approximately 10-15 mole % H_2O may not be observed during routine microthermometric investigations. It is therefore suggested that a CH_4-rich fluid, generated during the greenschist to amphibolite grade

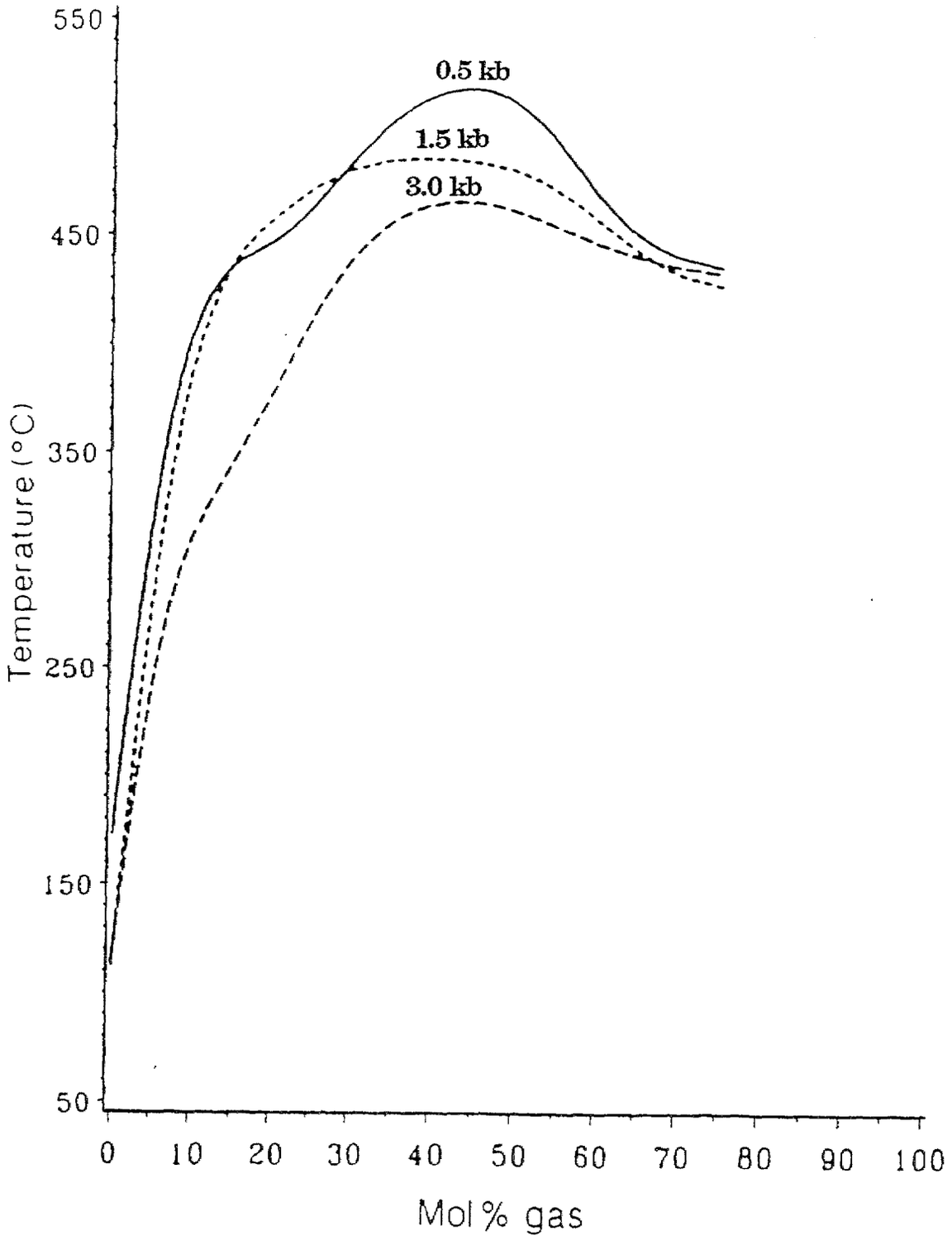

Figure 10. Temperature verses composition section for the CH4-H2O-NaCl (8 wt %) at 0.5 kbar (solid line), 1.5 kbar (short-dashed line) and 3.0 kbar (medium-dashed line) modified from Naden and Shepherd (1989). The two-phase region lies below the lines for all 3 pressures. Note that changes in pressure have only a limited effect on methane solubility at temperatures below 300°C.

metamorphism of the area, was present as the ambient fluid in the host rocks and that the CO_2-rich, ore-bearing? fluid was externally derived.

Although the above observations are based on a relatively small number of samples from selected deposits, they suggest a model involving deep, CO_2-rich (ore-bearing?) fluids of lower crustal or mantle origin. As these fluids ascend to the surface they undergo phase separation and mix with a reduced wallrock/metamorphic fluid to generate a CO_2/CH_4-rich fluid. Mixing of the more oxidised CO_2-rich fluids with the CH_4-rich fluids would provide an efficient means of reducing the gold complexes in the ore fluids and also for precipitating the sulfide minerals. The relative timing of fluid mixing and phase separation (boiling) is not certain but the observation of non-aqueous $CO_2 + CH_4$ inclusions suggests that phase separation may have occurred after fluid mixing. Furthermore, the extensive two-phase field for the system H_2O-CH_4-NaCl (Figure 10) indicates that fluids containing more than a few more percent CH_4 will experience significant unmixing over a wide range of geological conditions which would act as a trigger for gold deposition.

REFERENCES

Brown P.E. and Lamb W.M. (1989) P-V-T properties of fluids in the system H_2O-CO_2-NaCl: New graphical presentations and implications for fluid inclusion studies. *Geochim. Cosmochim. Acta*, **53**, 1209-1221.

Clark M.E., Archibald N.J. and Hodgson C.J. (1986) The structural and metamorphic setting of the Victory Gold Mine, Kambalda, Western Australia. In: MacDonald A.J. (editor), *Proceedings Gold '86, An international symposium on the geology of gold*, Toronto, Konsult International, p. 243-254.

Clark M.E., Carmichael D.M. and Hodgson C.J. (1988) Metasomatic processes and T-X_{CO2} conditions of wall rock alteration, Victory Gold Mine, Kambalda, Western Australia. In: Goode A.D.T. and Bosma L.I. (Compilers), *Bicentennial Gold '88 (extended abstracts, oral programme)*, Geological Society of Australia Abstract Series, **22**, 230- 234.

Cowden A. and Roberts D.E. (1990) Komatiite hosted nickel sulfide deposits, Kambalda. In: Hughes F.E. (Editor), *Geology of the Mineral Deposits of Australia and Papua New Guinea*, Australian Institute of Mining and Metallurgy, Melbourne, p. 567-581.

Eugster H.P. and Skippen G.B. (1967) Igneous and metamorphic reactions involving gas equilibria. In: Ableson P.H. (Editor) *Researches in Geochemistry*, Vol. 2, Wiley and Sons, New York, pp.492-520.

French B.M. (1966) Some geological implications of equilibrium between graphitè and C-H-O gas phase at high temperatures and pressures. *Rev. Geophys.*, **4**, 223-253.

Frey M., Bucher K. and Mullis J. (1980) Alpine metamorphism along the Geotraverse Based-Chaisso -- a review. *Eclogae Geol. Helv.*, **73**, 527-546.

Garba I. and Akande S.O. (1992) The origin and significance of non-aqueous CO_2 fluid inclusions in the auriferous veins of Bin Yauri, northwestern Nigeria. *Mineral. Deposita*, **27**, 249-255.

Ho S.E. (1987) Fluid inclusions: their potential as an exploration tool for Archaean gold deposits. In: Ho S.E. and Groves D.I. (editors), *Recent Advances in Understanding Precambrian Gold Deposits*. Geology Department and university Extension, The University of Western Australia, Publication **11**, 239-263..PA .PA

Ho S.E., Bennett J.M., Cassidy K.F., Hronsky J.M.A., Mikucki E.J. and Sang J.H. (1990) Nature of ore fluid, and transportational and depositional conditions in sub- amphibolite facies deposits. In: Ho S.E., Groves D.I. and Bennett J.M. (editors), *Gold Deposits of the Archaean Yilgarn Block, Western Australia: Nature, Genesis and Exploration Guides*. Geology Department and University Extension, The University of Western Australia, Publication **20**, 198-211.

Holloway J.R. (1981) Compositions and volumes of supercritical fluids in the earth's crust. In: Hollister L.S. and Crawford M.L. (editors), *Fluid Inclusions: Applications To Petrology*. Mineralogical Association of Canada Shortcourse Handbook **6**, p.13-38.

Hoschek G. (1973) Die reaktion Plogopit + Calcit + Quartz + Tremolit + H_2O + CO_2. *Contrib. Mineral. Petrol.*, **39**, 231-237.

Naden J. and Shepherd T.J. (1989) Role of methane and carbon dioxide in gold deposition. *Nature*, **342**, 793-795.

Phillips G.N. (1986) Geology and alteration in the Golden Mile, Kalgoorlie. *Econ. Geol.*, **81**, 779-808.

Phillips G.N. and Groves D.I. (1984) Fluid access and fluid-wallrock interaction in the genesis of the Archaean gold-quartz vein deposit at the Hunt mine, Kambalda, Western Australia. In: Foster R.P. (editor), *Gold '82: The Geology, Geochemistry and Genesis of Gold Deposits.* Special Publication Geological Society Zimbabwe No.**1**, A.A. Balkema, Rotterdam, p.389-416.

Smith T.J., Cloke P.L. and Kesler S.E. (1984) Geochemistry of fluid inclusions from the McIntyre-Hollinger gold deposit, Timmins, Ontario, Canada. *Econ. Geol.*, **79**, 1265- 1285.

Thomas A.V. and Spooner E.T.C. (1988) Fluid inclusions in the system H_2O-CH_4-NaCl-CO_2 from metasomatic tourmaline within the border unit of the Tanco zoned granitic pegmatite, S.E. Manitoba. *Geochim. Cosmochim. Acta*, **52**, 1065-1075.

Witt W.K. (1991) Regional metamorphic controls on alteration associated with gold mineralization in the Eastern Goldfields province, Western Australia: Implications for the timing and origin of Archean lode-gold deposits. *Geology*, **19**, 982-985.

Woodward H.P. (1906) Auriferous deposits and mines, North Coolgardie Goldfield. *Geological Survey of Western Australia Bulletin*, **22**, 92pp.

APPENDIX A

MICROTHERMOMETRIC DATA

Gold Deposits Associated with Alteration Assemblage 1

BINDULI

Sample Number	Inclusion Type	Size microns	Vol. % CO_2(L+V)	Vol. % H_2O vap.	Vol. % Solids	T_m CO_2	T_e	T_m ice	T_m clath	Salinity Wt% NaCl	Th CO_2	T_h	T_d	Density $g.cm^{-3}$	Comments
Binduli	E	12	95			-56.5			7.7	4.9	30.3			0.58	Sec 1st fracture, Th(L)
100872	E	10	95			-56.6			7.5	5.3	29.7			0.61	Sec 1st fracture, Th(L)
	E	8	95			-56.6			7.7	4.9	30.4			0.58	Sec 1st fracture, Th(L)
	E	6	95			-56.5			7.6	5.1	30.3			0.58	Sec 1st fracture, Th(L)
	E	10	95			-56.6			7.8	4.7	29.7			0.61	Sec 1st fracture, Th(L)
	H	5	100			-56.9					23.2			0.74	Sec 2nd fracture, Th(L)
	H	5	100			-56.9					12.3			0.84	Sec 2nd fracture, Th(L)
	H	5	100			-56.9					12.7			0.84	Sec 2nd fracture, Th(L)
	H	5	100			-56.9					14.0			0.83	Sec 2nd fracture, Th(L)
	E	8	95			-56.8			7.6		22.8			0.74	Sec 2nd fracture, Th(L)
	E	8	95			-56.7			7.5		15.5			0.82	Sec 2nd fracture, Th(L)
	E	6	95			-56.5			7.6		17.1			0.80	Sec 2nd fracture, Th(L)
	H	10	100			-56.5					20.3			0.77	Pseudosecondary, Th(L)
	H	15	100			-56.5					23.3			0.73	Pseudosecondary, Th(L)
	G	20	100			-56.6					2.2			0.91	Sec nucleated bubble,Th(L)
	G	20	100			-56.5					7.6			0.88	Sec nucleated bubble,Th(L)
	G	5	100			-56.6					7.6			0.88	Sec nucleated bubble,Th(L)
	G	15	100			-56.6					6.3			0.89	Sec nucleated bubble,Th(L)
	G	25	100			-56.5					6.8			0.88	Sec nucleated bubble,Th(L)
	G	10	100			-56.5					12.2			0.84	Sec nucleated bubble,Th(L)
	G	15	100			-56.6					20.4			0.77	Sec nucleated bubble,Th(L)
	G	8	100			-56.5					17.6			0.80	Sec nucleated bubble,Th(L)
	G	15	100			-56.6					22.9			0.74	Sec nucleated bubble,Th(L)
	G	5	100			-56.5					22.1			0.75	Sec nucleated bubble,Th(L)

HAWKINS FIND

Sample Number	Inclusion Type	Size microns	Vol. % CO_2(L+V)	Vol. % H_2O vap.	Vol. % Solids	T_m CO_2	T_e	T_m ice	T_m clath	Salinity Wt% NaCl	Th CO_2	T_h	T_d	Density $g.cm^{-3}$	Comments
Hawkins Find															
93961	C	18		10	2		-23.6	-3.9		6.3		184.7			Primary in quartz Th(L)
	C	20		10	2		-23.4	-4.0		6.5		198.2			Primary in quartz Th(L)
	C	15		10	2		-23.2	-4.1		6.6		221.5			Primary in quartz Th(L)
	C	10		10	2		-23.5	-3.6		5.9		180.6			Primary in quartz Th(L)
	C	12		10	2		-25.1	-3.8		6.2		195.2			Primary in quartz Th(L)
	B	20		10			-24.3	-4.0		6.5		201.0			Primary in quartz Th(L)
	B	10		10				-3.9		6.3		241.2			Primary in quartz Th(L)

Sample Number	Inclusion Type	Size microns	Vol. % CO_2(L+V)	Vol. % H_2O vap.	Vol. % Solids	T_m CO_2	T_e	T_m ice	T_m clath	Salinity Wt% NaCl	Th CO_2	T_h	T_d	Density $g.cm^{-3}$	Comments
Hawkins Find 93961	B	15		5				-3.9		6.3		186.4			Pseudosecondary in qtz
	B	8		10			-23.8	-3.3		5.4		193.2			Pseudosecondary in qtz
	C	5		10	2		-24.2	-3.4		5.6		202.2			Pseudosecondary in qtz
	B	5		10			-23.9	-3.9		6.3		198.2			Pseudosecondary in qtz
	B	5		10				-4.1		6.6		206.6			Pseudosecondary in qtz
	B	10		25					11.3				260		Secondary in albite
	B	5		25					11.2		278.2				Secondary in albite, Th(L)
	B	3		25					11.0		283.4				Secondary in albite, Th(L)
	B	3		20					11.1		286.5				Secondary in albite, Th(L)
	B	2		25					11.0		287.6				Secondary in albite, Th(L)
	B	10		25					10.9				240		Secondary in albite
	B	5		20					11.0		297.2				Secondary in albite, Th(L)
	B	3		25					11.2		287.4				Secondary in albite, Th(L)
	B	3		20					11.4		288.9				Secondary in albite, Th(L)
	B	3		25					10.9		288.0				Secondary in albite, Th(L)
	B	30		5							243.9				Secondary, Th(L)
	B	10		10							202.0				Secondary, Th(L)
	B	8		5							190.5				Secondary, Th(L)
	B	6		5							173.6				Secondary, Th(L)
	B	10		10							235.8				Secondary, Th(L)

Gold Deposits Associated with Alteration Assemblage 2

GOONGARRIE

Sample Number	Inclusion Type	Size microns	Vol. % CO_2(L+V)	Vol. % H_2O vap.	Vol. % Solids	T_m CO_2	T_e	T_m ice	T_m clath	Salinity Wt% NaCl	Th CO_2	T_h	T_d	Density $g.cm^{-3}$	Comments
Goongarrie 98152	H	10	100			-57.3					23.4			0.73	Secondary Th(L)
	H	8	100			-57.2					22.1			0.75	Secondary Th(L)
	H	8	100			-57.4					20.7			0.77	Secondary Th(L)
	H	6	100			-57.3					18.7			0.79	Secondary Th(L)
	H	6	100			-57.6					16.8			0.81	Secondary Th(L)
	H	5	100			-57.3					16.5			0.81	Secondary Th(L)
	G	10	100			-66.1									Sec, sublimation to vapor
	G	8	100												Sec, sublimation to vapor
	G	4	100			-57.0					17.6			0.80	Pseudosecondary Th(L)
	G	5	100			-57.1									Pseudosec sublimation to va
	G	4	100			-57.0									Pseudosec sublimation to va
	G	3	100			-57.1									Pseudosec sublimation to va

Gold Deposits Associated with Alteration Assemblage 3

SAND KING

Sample Number	Inclusion Type	Size microns	Vol. % CO_2(L+V)	Vol. % H_2O vap.	Vol. % Solids	T_m CO_2	T_e	T_m ice	T_m clath	Salinity Wt% NaCl	Th CO_2	T_h	T_d	Density g.cm^{-3}	Comments
Sand King	E	15	50			-59.2					20.2			0.77	Secondary
98151A	E	8	70			-57.5					22.1			0.75	Secondary
	H	5	100			-57.2					21.8			0.75	Secondary
	H	8	100			-57.6					22.2			0.75	Secondary
	G	20	100			-57.2									Secondary
	H	5	100			-56.9					23.1			0.74	Secondary
	H	15	100			-57.2					24.8			0.71	Secondary
	E	20	40			-57.2									Secondary
	H	20	100			-57.2					27.3			0.67	Secondary
	H	10	100			-57.2					26.5			0.69	Secondary
	E	10	50			-57.3					8.0			0.88	Secondary
	A	20	60			-60.9					-3.2			0.95	Secondary
	A	10	80			-59.8									Secondary
	A	5	50			-60.7									Secondary
	A	5	50			-60.3									Secondary
	E	10	20									300.1			Secondary Th(L)
	E	8	50									297.7			Secondary Th(L)
	E	8	80									295.5			Secondary Th(L)
	E	20	80									343.5			Secondary Th(L)
	B	5		10								221.9			Secondary Th(L)
	B	5		10								268.2			Secondary Th(L)
	A?	10	50									284.5			Secondary Th(L)
	A?	5	60									310.8			Secondary Th(L)
	A?	4	40									298.6			Secondary Th(L)

MISSOURI

Sample Number	Inclusion Type	Size microns	Vol. % CO_2(L+V)	Vol. % H_2O vap.	Vol. % Solids	T_m CO_2	T_e	T_m ice	T_m clath	Salinity Wt% NaCl	Th CO_2	T_h	T_d	Density g.cm^{-3}	Comments
Missouri	H	20	100			-56.9					18.9			0.79	Secondary Th(L)
98152	H	20	100			-56.5					20.2			0.77	Secondary Th(L)
	H	10	100			-56.5					27.1			0.68	Secondary Th(L)
	H	20	100			-56.6					23.9			0.73	Secondary Th(L)
	H	8	100			-56.7					28.2			0.65	Secondary Th(L)
	H	8	100			-56.5					18.9			0.79	Secondary Th(L)
	H	5	100			-56.5					27.4			0.67	Secondary Th(L)
	H	20	100			-56.6					25.6			0.70	Secondary Th(L)
	H	5	100			-56.5					26.3			0.69	Secondary Th(L)
	H	5	100			-56.6					15.2			0.82	Secondary Th(L)
	H	3	100			-56.5					26.9			0.68	Secondary Th(L)
	H	8	100			-56.4					29.6			0.61	Secondary Th(L)
	G	10	100			-56.5					18.6			0.79	Secondary Th(L)
	H	8	100			-56.5					28.9			0.63	Secondary Th(L)

Sample Number	Inclusion Type	Size microns	Vol. % CO_2(L+V)	Vol. % H_2O vap.	Vol. % Solids	T_m CO_2	T_e	T_m ice	T_m clath	Salinity Wt% NaCl	Th CO_2	T_h	T_d	Density $g.cm^{-3}$	Comments
Missouri 98152	B	10	50			-56.6			7.8	4.32	28.8			0.64	Secondary Th(L)
	G	10	100			-56.5					18.3			0.79	Secondary Th(L)
	A	10	80			-56.5					20.2			0.77	Secondary Th(L)
	G	5	100			-56.6					8.9			0.87	Secondary Th(L)
	G	5	100			-56.5					15.9			0.81	Secondary Th(L)
	G	15	100			-56.6					16.9			0.80	Secondary Th(L)
	G	10	100			-60.7					17.6			0.80	Secondary Th(L)
	G	10	100			-56.6					12.9			0.84	Secondary Th(L)
	G	10	100			-56.5					12.7			0.84	Secondary Th(L)
	G	5	100			-56.5					14.4			0.83	Secondary Th(L)
	G	20	100			-57.6					20.8			0.77	Secondary Th(L)
	G	10	100			-57.3					18.4			0.79	Secondary Th(L)
	G	10	100			-57.4					11.1			0.85	Secondary Th(L)
	G	8	80			-57.3					12.3			0.84	Secondary Th(L)
	G	5	100			-57.5					13.1			0.84	Secondary Th(L)
	G	5	100			-57.5					18.0			0.79	Secondary Th(L)
	G	5	100			-57.6					1.6			0.92	Secondary Th(L)
	G	5	100			-57.5					20.7			0.77	Secondary Th(L)
	G	5	100			-57.5					23.0			0.74	Secondary Th(L)
	G	5	100			-57.5					0.3			0.93	Secondary Th(L)
	G	5	100			-57.5					0.5			0.93	Secondary Th(L)

BONNIE DOON

Sample Number	Inclusion Type	Size microns	Vol. % CO_2(L+V)	Vol. % H_2O vap.	Vol. % Solids	T_m CO_2	T_e	T_m ice	T_m clath	Salinity Wt% NaCl	Th CO_2	T_h	T_d	Density $g.cm^{-3}$	Comments
Bonnie	A	20	20			-57.1			7.4	5.05	23.7		230	0.73	Secondary ThCO2(L)
Doone	A	30	20			-57.1			7.8	4.32	18.7		176.4	0.79	Secondary ThCO2(L)
98154	E	5	30			-57.3					27.6		230	0.67	Secondary ThCO2(L)
	E	8	30			-57.2					27.2		240	0.67	Secondary ThCO2(L)
	G	8	100									136.1	230		Secondary Th(L)
	G	6	100									136.5	220		Secondary Th(L)
	H	5	100			-57.1							240		Secondary Th(L)
	E	20	30			-56.5					26.9			0.68	Secondary Th(L)
	B	10	10			-56.5			7.8	4.32	31.2			0.47	Secondary Th(L)
	B	4	10								31.0			0.52	Secondary Th(L)
	B	3	10									252.4			Secondary Th(L)
	B	4	10												Secondary
	B	5	10												Secondary
	B	8	5								30.8			0.55	Secondary Th(L)
	B	10	5												Secondary
	B	8	5												Secondary Th(L)

SUNDAY GIFT

Sample Number	Inclusion Type	Size microns	Vol. % CO_2(L+V)	Vol. % H_2O vap.	Vol. % Solids	T_m CO_2	T_e	T_m ice	T_m clath	Salinity Wt% NaCl	Th CO_2	T_h	T_d	Density $g.cm^{-3}$	Comments
Sunday	G	6	100			-56.5									Secondary
Gift	G	3	100			-56.5									Secondary
100845	G	6	100			-56.6									Secondary
	G	4	100			-56.5									Secondary
	H	3	100			-56.6					28.8			0.64	Secondary Th(L)
	H	2	100			-56.6					18.3			0.79	Secondary Th(L)
	H	1	100			-56.5					18.7			0.79	Secondary Th(L)
	H	6	100			-56.9					29.4			0.62	Secondary Th(L)
	G	10	100			-57.0									Secondary
	G	10	100			-56.9									Secondary
	H	6	100			-56.8					30.9			0.54	Secondary Th(L)
	H	6	100			-56.6					29.6			0.61	Secondary Th(L)
	H	5	100			-57.0					29.8			0.61	Secondary Th(L)
	H	3	100			-56.9					29.5			0.62	Secondary Th(L)

GOODENOUGH

Sample Number	Inclusion Type	Size microns	Vol. % CO_2(L+V)	Vol. % H_2O vap.	Vol. % Solids	T_m CO_2	T_e	T_m ice	T_m clath	Salinity Wt% NaCl	Th CO_2	T_h	T_d	Density $g.cm^{-3}$	Comments
Goodenough	G	5	100			-60.9					-20.7			1.04	Pseudo-secondary Th(L)
100846	G	3	100			-61.2					3.4			0.91	Pseudo-secondary Th(L)
	G	5	100			-61.7					-18.3			1.02	Pseudo-secondary Th(L)
	G	5	100			-61.0					9.6			0.86	Pseudo-secondary Th(L)
	G	10	100			-60.9					13.8			0.83	Pseudo-secondary Th(L)
	G	10	100			-61.1					6.3			0.89	Pseudo-secondary Th(L)
	G	15	100			-65.4					-6.2			0.96	Secondary Th(L)
	G	5	100			-63.0					9.1			0.87	Secondary Th(L)
	G	10	100			-63.5					6.9			0.88	Secondary Th(L)
	G	10	100			-63.9					8.2			0.87	Secondary Th(L)

YUNDAGA

Sample Number	Inclusion Type	Size microns	Vol. % CO_2(L+V)	Vol. % H_2O vap.	Vol. % Solids	T_m CO_2	T_e	T_m ice	T_m clath	Salinity Wt% NaCl	Th CO_2	T_h	T_d	Density $g.cm^{-3}$	Comments
Yundaga	C	20	60		2	-59.4					13.6			0.83	Secondary Th(L)
100840	G	20	100			-59.5					20.6			0.77	Secondary Th(L)
	C	30	75		2	-59.4					15.4			0.82	Secondary Th(L)
	G	8	100			-59.7					3.9			0.90	Secondary Th(L)
	H	8	100			-61.7					5.5			0.89	Secondary Th(L)
	G	6	100			-60.4					-14.3			1.01	Secondary Th(L)
	A	8	90			-62.0					-14.5			1.01	Secondary Th(L)
	A	10	80			-63.3			-1.1	16.80	7.8			0.88	Secondary Th(L)

Sample Number	Inclusion Type	Size microns	Vol. % CO_2(L+V)	Vol. % H_2O vap.	Vol. % Solids	T_m CO_2	T_e	T_m ice	T_m clath	Salinity Wt% NaCl	Th CO_2	T_h	T_d	Density g.cm^{-3}	Comments
Yundaga	A	12	80			-63.0			-1.0	16.69	-7.5			0.97	Secondary Th(L)
100840	G	15	100			-63.7					21.9			0.75	Secondary Th(L)
	G	15	100			-63.5					21.2			0.76	Secondary Th(L)
	H	5	100			-62.9									
	A	20	40						-1.0	16.69					
	H	5	100			-63.3									
	B	10	10									198.3			Secondary Th(L)
	B	6	25									252.8			Secondary Th(L)
	B	6	25									252.3			Secondary Th(L)
	B	3	25									123.7			Secondary Th(L)
	B	20	20									232.2			Secondary Th(L)
	B	10	10									191.5			Secondary Th(L)
	A	10	90										353.0		Secondary
	A	10	75										313.0		Secondary
	A	10	40										337.0		Secondary
	A	10	40										397.0		Secondary
	B	2	20												Secondary
	B	2	30										380		Secondary
	A	5	90									408.9			Secondary Th(L)

LADY HARRIET

Sample Number	Inclusion Type	Size microns	Vol. % CO_2(L+V)	Vol. % H_2O vap.	Vol. % Solids	T_m CO_2	T_e	T_m ice	T_m clath	Salinity Wt% NaCl	Th CO_2	T_h	T_d	Density g.cm^{-3}	Comments
Lady	G	4	100			-58.9					7.3			0.88	Pseudo-sec Th(L)
Harriet	G	6	100			-59.1					18.0			0.79	Pseudo-sec Th(L)
100835	A	10	30				-22.8		8.8						Pseudo-sec Th(L)
	B	5		5					9.1						Pseudo-sec Th(L)
	G	6	100			-58.9					9.2			0.87	Pseudo-sec Th(L)
	H	5	100			-59.0					21.2			0.76	Pseudo-sec Th(L)
	H	4	100			-58.9					22.3			0.75	Pseudo-sec Th(L)
	H	5	100			-58.2					20.1			0.77	Pseudo-sec Th(L)
	H	10	100			-58.1			8.1		20.3			0.77	Pseudo-sec Th(L)
	G	5	100			-58.0			8.7		18.3			0.79	Pseudo-sec Th(L)
	G	3	100			-58.1					20.4			0.77	Pseudo-sec Th(L)
	B	5			5		-25	-5.3		8.3		253.8			Secondary Th(L)
	B	4			5		-30	-5.1		8.0		209.3			Secondary Th(L)
	B	10			5		-30	-5.5		8.6		219.2			Secondary Th(L)
	B	8			5		-28	-3.3		5.4		80.8			Secondary Th(L)
	B	10			5		-29	-5.3		8.3		186.5			Secondary Th(L)
	B	4			5		-28	-5.2		8.2		243.3			Secondary Th(L)
	B	4			5		-30	-5.0		7.9		187.9			Secondary Th(L)
	B	5			5		-26	-4.5		7.2		188.6			Secondary Th(L)

LADY SHENTON

Sample Number	Inclusion Type	Size microns	Vol. % CO_2(L+V)	Vol. % H_2O vap.	Vol. % Solids	T_m CO_2	T_e	T_m ice	T_m clath	Salinity Wt% NaCl	Th CO_2	T_h	T_d	Density $g.cm^{-3}$	Comments
Lady Shenton 100806	H	10	100			-57.9					22.4			0.75	Pseudo-secondary Th(L)
	H	5	100			-57.8					21.7			0.75	Pseudo-secondary Th(L)
	G	6	100			-58.5					16.7			0.81	Pseudo-secondary Th(L)
	G	8	100			-58.0					15.5			0.82	Pseudo-secondary Th(L)
	G	4	100			-57.9					17.2			0.80	Pseudo-secondary Th(L)
	G	4	100			-58.3					15.3			0.82	Pseudo-secondary Th(L)
	G	4	100			-57.6					16.6			0.81	Pseudo-secondary Th(L)
	H	3	100			-57.9					21.6			0.76	Pseudo-secondary Th(L)
	H	10	100			-58.0					23.5			0.73	Pseudo-secondary Th(L)
	H	3	100			-57.9					7.6			0.88	Pseudo-secondary Th(L)
	H	5	100			-58.1					22.3			0.75	Pseudo-secondary Th(L)
	G	10	100			-58.8					17.9			0.80	Pseudo-secondary Th(L)
	G	3	100			-58.6					15.4			0.82	Pseudo-secondary Th(L)
	G	5	100			-58.5					16.2			0.81	Pseudo-secondary Th(L)
	G	5	100			-58.9					12.4			0.84	Pseudo-secondary Th(L)
	G	5	100			-58.8					19.4			0.78	Pseudo-secondary Th(L)
	G	4	100			-58.5					16.4			0.81	Pseudo-secondary Th(L)
	G	3	100			-58.6					20.7			0.77	Pseudo-secondary Th(L)

ASPACIA

Sample Number	Inclusion Type	Size microns	Vol. % CO_2(L+V)	Vol. % H_2O vap.	Vol. % Solids	T_m CO_2	T_e	T_m ice	T_m clath	Salinity Wt% NaCl	Th CO_2	T_h	T_d	Density $g.cm^{-3}$	Comments
Aspacia 98244	G	5	100			-59.8					1.3			0.92	Pseudo-secondary, Th(L), #1
	G	5	100			-59.9					-2.0			0.94	Pseudo-secondary, Th(L), #1
	G	3	100			-59.6					-14.2			1.00	Pseudo-secondary, Th(L), #1
	G	2	100			-59.8					-15.7			1.01	Pseudo-secondary, Th(L), #1
	G	5	100			-59.9					-12.5			1.00	Pseudo-secondary, Th(L), #1
	G	5	100			-57.6					-7.2			0.97	Secondary Th(L)
	G	3	100			-57.7					-7.3			0.97	Secondary Th(L)
	G	4	100			-57.5					-12.0			0.99	Secondary Th(L)
	G	6	100								-0.4			0.93	Did not freeze
	G	7	100								-0.4			0.93	Did not freeze
	G	4	100			-57.6					-10.9			0.99	Secondary Th(L)
	G	2	100			-57.4					-1.5			0.94	Secondary Th(L)
	G	3	100			-57.6					6.3			0.89	Secondary Th(L)

Gold Deposits Associated with Alteration Assemblage 4

ST ALBANS

Sample Number	Inclusion Type	Size microns	Vol. % CO_2(L+V)	Vol. % H_2O vap.	Vol. % Solids	T_m CO_2	T_e	T_m ice	T_m clath	Salinity Wt% NaCl	Th CO_2	T_h	T_d	Density $g.cm^{-3}$	Comments
St Albans	A	50	35				-58	-15.9		23.2					Secondary in epidote Th(L)
98222	A	25	30						14.1			361.4			Secondary in epidote Th(L)
	B	10	10						10.7			227.9			Secondary in epidote Th(L)
	B	50	5				-59	-24.8		25.9					Secondary in epidote Th(L)
	B	20	5				-58	-24.6		25.7		254.8			Secondary in epidote Th(L)
	A	25	75						9.5			341.0			Secondary in epidote Th(L)
	A	15	80						10.7						Secondary in epidote Th(L)
	A	25	60			-112.7			10.7			355.6			Secondary in epidote Th(L)
	C	20	15		3			-0.8	5.4			286.3			Secondary in epidote Th(L)
	B	30	10					-0.8				247.0			Secondary in epidote Th(L)
	A	60	30					-0.8	10.6				275.9		Secondary in epidote Th(L)
	C	50	15		5	-84.8		-0.8	5.5			293.6	330		Secondary in epidote Th(L)
	A	30	30					-0.8	5.4						Secondary in epidote Th(L)
	C	15	50		3			-0.8	5.3			232.8			Secondary in epidote Th(L)
	C	40	15		5			-0.8	5.3			301.0			Secondary in epidote Th(L)
	A	10	30					-0.8	5.5			331.6			Secondary in epidote Th(L)
	A	15	50					-12.1	13.4						Secondary in quartz Th(L)
	A	15	40						15.3						Secondary in quartz Th(L)
	A	5	50						14.0			327.6			Secondary in quartz Th(L)
	A	5	50						6.7			319.1			Secondary in quartz Th(L)
	A	5	40						6.9			290.4			Secondary in quartz Th(L)
	A	5	50						6.6			323.5			Secondary in quartz Th(L)

APPENDIX B

GAS RATIOS IN THE VAPOUR PHASE FROM RAMAN MICROPROBE ANALYSIS

Gold Deposits Associated with Alteration Assemblage 1

HAWKINS FIND

Sample Number	SO_2 mol %	CO_2 mol %	N_2 mol %	H_2S mol %	CH_4 mol %	C_2H_6 mol %	C_3H_8 mol %	H_2 mol %	Comments
93958	0	46	12	0	42	0	0	0	Type B
93958	0	6	8	0	85	0	0	0	Type C
93958	0	0	49	0	51	0	0	0	Type B
93958	0	0	33	0	67	0	0	0	type B

Gold Deposits Associated with Alteration Assemblage 2

GOONGARRIE

Sample Number	SO_2 mol %	CO_2 mol %	N_2 mol %	H_2S mol %	CH_4 mol %	C_2H_6 mol %	C_3H_8 mol %	H_2 mol %	Comments
93927	0	100	0	0	0	0	0	0	Type H 12 um
93927	0	100	0	0	0	0	0	0	Type G
93927	0	100	0	0	0	0	0	0	Type G
93927	0	100	0	0	0	0	0	0	Type H 10 um
93927	0	100	0	0	0	0	0	0	Type G
93927	0	100	0	0	0	0	0	0	Type G

Gold Deposits Associated with Alteration Assemblage 3

SAND KING

Sample Number	SO_2 mol %	CO_2 mol %	N_2 mol %	H_2S mol %	CH_4 mol %	C_2H_6 mol %	C_3H_8 mol %	H_2 mol %	Comments
98151A	0	100	0	0	0	0	0	0	Type H 10um liquid phase
98151A	0	100	0	0	0	0	0	0	Type G 10um gas phase
98151A	0	100	0	0	0	0	0	0	Type A 50% vap.
98151A	0	79	0	0	21	0	0	0	Type A in undeformed quartz
98151A	0	75	0	0	25	0	0	0	Type A 75% vap
98151A	0	60	0	0	36	0	4	0	Type A 70% vap

MISSOURI

Sample Number	SO_2 mol %	CO_2 mol %	N_2 mol %	H_2S mol %	CH_4 mol %	C_2H_6 mol %	C_3H_8 mol %	H_2 mol %	Comments
98152A	0	100	0	0	0	0	0	0	Type G 100% vap
98152A	0	97	0	0	3	0	0	0	Type H Liquid phase
98152A	0	100	0	0	0	0	0	0	Type G 100% vapour
98152A	0	0	0	0	100	0	0	0	Type G 100% vapour

BONNIE DOON

Sample Number	SO_2 mol %	CO_2 mol %	N_2 mol %	H_2S mol %	CH_4 mol %	C_2H_6 mol %	C_3H_8 mol %	H_2 mol %	Comments
98154	0	53	0	0	47	0	0	0	Type A 30% vapour
98154	0	59	0	0	41	0	0	0	Type A 30% vapour
98154	0	94	0	0	6	0	0	0	Type E 25% vapour
98154	0	94	0	0	6	0	0	0	Type E 20% vapour

SUNDAY GIFT

Sample Number	SO_2 mol %	CO_2 mol %	N_2 mol %	H_2S mol %	CH_4 mol %	C_2H_6 mol %	C_3H_8 mol %	H_2 mol %	Comments
100846	0	73	0	0	27	0	0	0	Type G 100% vapour
100846	0	5	0	0	95	0	0	0	Type G 100% vapour
100846	0	6	0	0	94	0	0	0	Type G 100% vapour
100846	0	85	0	0	15	0	0	0	Type G 100% vapour
100846	0	76	0	0	24	0	0	0	Type G 100% vapour
100846	0	88	0	0	12	0	0	0	Type G 100% vapour

LADY SHENTON

Sample Number	SO_2 mol %	CO_2 mol %	N_2 mol %	H_2S mol %	CH_4 mol %	C_2H_6 mol %	C_3H_8 mol %	H_2 mol %	Comments
100806	0	82	0	0	18	0	0	0	Type G, 30um
100806	0	67	0	0	33	0	0	0	Type G, 15um
100806	0	47	0	0	53	0	0	0	Type G, 12um
100806	0	90	0	0	10	0	0	0	Type G, 10um

Gold Deposits Associated with Alteration Assemblage 4

ST ALBANS

Sample Number	SO_2 mol %	CO_2 mol %	N_2 mol %	H_2S mol %	CH_4 mol %	C_2H_6 mol %	C_3H_8 mol %	H_2 mol %	Comments
98222	0	0	0	0	100	0	0	0	Type B 60um 5% vapour in epidote
98222	0	0	0	0	100	0	0	0	Type A 10um 40% vapour in epidote
98222	0	0	0	0	100	0	0	0	Type C, 4 solids + calcite, 15% vap
98222	0	0	0	0	100	0	0	0	Type A, 40% vapour in epidote
98222	0	0	0	0	100	0	0	0	Type B, 10% vapour in epidote
98222	0	0	0	0	100	0	0	0	Type A, 95% vapour in quartz